13. NEUTRINO MASS, MIXING, AND OSCILLATIONS

Written May 2010 by K. Nakamura (IPMU, U. Tokyo, KEK) and S.T. Petcov (SISSA/INFN Trieste, IPMU, U. Tokyo, Bulgarian Academy of Sciences).

The experiments with solar, atmospheric, reactor and accelerator neutrinos have provided compelling evidences for oscillations of neutrinos caused by nonzero neutrino masses and neutrino mixing. The data imply the existence of 3-neutrino mixing in vacuum. We review the theory of neutrino oscillations, the phenomenology of neutrino mixing, the problem of the nature - Dirac or Majorana, of massive neutrinos, the issue of CP violation in the lepton sector, and the current data on the neutrino masses and mixing parameters. The open questions and the main goals of future research in the field of neutrino mixing and oscillations are outlined.

13.1. Introduction: Massive neutrinos and neutrino mixing

It is a well-established experimental fact that the neutrinos and antineutrinos which take part in the standard charged current (CC) and neutral current (NC) weak interaction are of three varieties (types) or flavours: electron, ν_e and $\bar{\nu}_e$, muon, ν_μ and $\bar{\nu}_\mu$, and tauon, ν_τ and $\bar{\nu}_\tau$. The notion of neutrino type or flavour is dynamical: ν_e is the neutrino which is produced with e^+, or produces an e^- in CC weak interaction processes; ν_μ is the neutrino which is produced with μ^+, or produces μ^-, *etc.* The flavour of a given neutrino is Lorentz invariant. Among the three different flavour neutrinos and antineutrinos, no two are identical. Correspondingly, the states which describe different flavour neutrinos must be orthogonal (within the precision of the corresponding data): $\langle\nu_{l'}|\nu_l\rangle = \delta_{l'l}$, $\langle\bar{\nu}_{l'}|\bar{\nu}_l\rangle = \delta_{l'l}$, $\langle\bar{\nu}_{l'}|\nu_l\rangle = 0$.

It is also well-known from the existing data (all neutrino experiments were done so far with relativistic neutrinos or antineutrinos), that the flavour neutrinos ν_l (antineutrinos $\bar{\nu}_l$), are always produced in weak interaction processes in a state that is predominantly left-handed (LH) (right-handed (RH)). To account for this fact, ν_l and $\bar{\nu}_l$ are described in the Standard Model (SM) by a chiral LH flavour neutrino field $\nu_{lL}(x)$, $l = e, \mu, \tau$. For massless ν_l, the state of ν_l ($\bar{\nu}_l$) which the field $\nu_{lL}(x)$ annihilates (creates) is with helicity (-1/2) (helicity +1/2). If ν_l has a non-zero mass $m(\nu_l)$, the state of ν_l ($\bar{\nu}_l$) is a linear superposition of the helicity (-1/2) and (+1/2) states, but the helicity +1/2 state (helicity (-1/2) state) enters into the superposition with a coefficient $\propto m(\nu_l)/E$, E being the neutrino energy, and thus is strongly suppressed. Together with the LH charged lepton field $l_L(x)$, $\nu_{lL}(x)$ forms an $SU(2)_L$ doublet. In the absence of neutrino mixing and zero neutrino masses, $\nu_{lL}(x)$ and $l_L(x)$ can be assigned one unit of the additive lepton charge L_l and the three charges L_l, $l = e, \mu, \tau$, are conserved by the weak interaction.

At present there is no evidence for the existence of states of relativistic neutrinos (antineutrinos), which are predominantly right-handed, ν_R (left-handed, $\bar{\nu}_L$). If RH neutrinos and LH antineutrinos exist, their interaction with matter should be much weaker than the weak interaction of the flavour LH neutrinos ν_l and RH antineutrinos $\bar{\nu}_l$, *i.e.*, ν_R ($\bar{\nu}_L$) should be "sterile" or "inert" neutrinos (antineutrinos) [1]. In the formalism of the Standard Model, the sterile ν_R and $\bar{\nu}_L$ can be described by $SU(2)_L$ singlet RH neutrino fields $\nu_R(x)$. In this case, ν_R and $\bar{\nu}_L$ will have no gauge interactions, *i.e.*, will not couple to the weak $W^\pm$ and Z^0 bosons. If present in an extension of the Standard Model, the RH neutrinos can play a crucial role i) in the generation of neutrino masses and mixing, ii) in understanding the remarkable disparity between the magnitudes of neutrino masses and the masses of the charged leptons and quarks, and iii) in the generation of the observed matter-antimatter asymmetry of the Universe (via the leptogenesis mechanism [2]) . In this scenario which is based on the see-saw theory [3], there is a link between the generation of neutrino masses and the generation of the baryon asymmetry of the Universe. The simplest hypothesis is that to each LH flavour neutrino field $\nu_{lL}(x)$ there corresponds a RH neutrino field $\nu_{lR}(x)$, $l = e, \mu, \tau$.

The experiments with solar, atmospheric and reactor neutrinos [4–16] have provided compelling evidences for the existence of neutrino oscillations [17,18], transitions in flight between the different flavour neutrinos ν_e, ν_μ, ν_τ (antineutrinos $\bar{\nu}_e$, $\bar{\nu}_\mu$, $\bar{\nu}_\tau$), caused by nonzero neutrino masses and neutrino mixing. Strong evidences for oscillations of muon neutrinos were obtained also in the long-baseline accelerator neutrino experiments K2K [20] and MINOS [21,22]. In addition, a short-baseline accelerator experiment LSND [23] observed a possible indication of $\bar{\nu}_\mu \to \bar{\nu}_e$ oscillations. If confirmed, this result required the existence of at least one additional neutrino type. More recently, MiniBooNE searched for $\nu_\mu \to \nu_e$ transitions, and if the neutrinos oscillate in the same way as antineutrinos, the MiniBooNE result [24] does not support the interpretation of the LSND data in terms of $\bar{\nu}_\mu \to \bar{\nu}_e$ oscillations.

The existence of flavour neutrino oscillations implies that if a neutrino of a given flavour, say ν_μ, with energy E is produced in some weak interaction process, at a sufficiently large distance L from the ν_μ source the probability to find a neutrino of a different flavour, say ν_τ, $P(\nu_\mu \to \nu_\tau; E, L)$, is different from zero. $P(\nu_\mu \to \nu_\tau; E, L)$ is called the $\nu_\mu \to \nu_\tau$ oscillation or transition probability. If $P(\nu_\mu \to \nu_\tau; E, L) \neq 0$, the probability that ν_μ will not change into a neutrino of a different flavour, *i.e.*, the "ν_μ survival probability" $P(\nu_\mu \to \nu_\mu; E, L)$, will be smaller than one. If only muon neutrinos ν_μ are detected in a given experiment and they take part in oscillations, one would observe a "disappearance" of muon neutrinos on the way from the ν_μ source to the detector. As a consequence of the results of the experiments quoted above the existence of oscillations or transitions of the solar ν_e, atmospheric ν_μ and $\bar{\nu}_\mu$, accelerator ν_μ (at $L \sim 250$ km and $L \sim 730$ km) and reactor $\bar{\nu}_e$ (at $L \sim 180$ km), driven by nonzero neutrino masses and neutrino mixing, was firmly established. There are strong indications that the solar ν_e transitions are affected by the solar matter [25,26].

Oscillations of neutrinos are a consequence of the presence of flavour neutrino mixing, or lepton mixing, in vacuum. In the formalism of local quantum field theory, used to construct the Standard Model, this means that the LH flavour neutrino fields $\nu_{lL}(x)$, which enter into the expression for the lepton current in the CC weak interaction Lagrangian, are linear combinations of the fields of three (or more) neutrinos ν_j, having masses $m_j \neq 0$:

$$\nu_{lL}(x) = \sum_j U_{lj}\, \nu_{jL}(x), \quad l = e, \mu, \tau, \tag{13.1}$$

where $\nu_{jL}(x)$ is the LH component of the field of ν_j possessing a mass m_j and U is a unitary matrix - the neutrino mixing matrix [1,17,18]. The matrix U is often called the Pontecorvo-Maki-Nakagawa-Sakata (PMNS) or Maki-Nakagawa-Sakata (MNS) mixing matrix. Obviously, Eq. (13.1) implies that the individual lepton charges L_l, $l = e, \mu, \tau$, are not conserved.

All existing neutrino oscillation data, except for the LSND result [23], can be described assuming 3-flavour neutrino mixing in vacuum. The data on the invisible decay width of the Z^0-boson is compatible with only 3 light flavour neutrinos coupled to Z^0 [19]. The number of massive neutrinos ν_j, n, can, in general, be bigger than 3, $n > 3$, if, for instance, there exist sterile neutrinos and they mix with the flavour neutrinos. It follows from the existing data that at least 3 of the neutrinos ν_j, say ν_1, ν_2, ν_3, must be light, $m_{1,2,3} \lesssim 1$ eV, and must have different masses, $m_1 \neq m_2 \neq m_3$. At present there are no compelling experimental evidences for the existence of more than 3 light neutrinos.

Being electrically neutral, the neutrinos with definite mass ν_j can be Dirac fermions or Majorana particles [27,28]. The first possibility is realised when there exists a lepton charge carried by the neutrinos ν_j, which is conserved by the particle interactions. This could be, *e.g.*, the total lepton charge $L = L_e + L_\mu + L_\tau$: $L(\nu_j) = 1$, $j = 1, 2, 3$. In this case the neutrino ν_j has a distinctive antiparticle $\bar{\nu}_j$: $\bar{\nu}_j$ differs from ν_j by the value of the lepton charge L it carries, $L(\bar{\nu}_j) = -1$. The massive neutrinos ν_j can be Majorana particles if no lepton charge is conserved (see, *e.g.*, Ref. 29). A massive Majorana particle χ_j is identical with its antiparticle $\bar{\chi}_j$: $\chi_j \equiv \bar{\chi}_j$. On the basis of the existing neutrino data it is impossible to determine whether the massive neutrinos are Dirac or Majorana fermions.

In the case of n neutrino flavours and n massive neutrinos, the $n \times n$ unitary neutrino mixing matrix U can be parametrised by $n(n-1)/2$ Euler angles and $n(n+1)/2$ phases. If the massive neutrinos ν_j are Dirac particles, only $(n-1)(n-2)/2$ phases are physical and can be responsible for CP violation in the lepton sector. In this respect the neutrino (lepton) mixing with Dirac massive neutrinos is similar to the quark mixing. For $n = 3$ there is just one CP violating phase in U, which is usually called "the Dirac CP violating phase." CP invariance holds if (in a certain standard convention) U is real, $U^* = U$.

If, however, the massive neutrinos are Majorana fermions, $\nu_j \equiv \chi_j$, the neutrino mixing matrix U contains $n(n-1)/2$ CP violation phases [30,31], *i.e.*, by $(n-1)$ phases more than in the Dirac neutrino case: in contrast to Dirac fields, the massive Majorana neutrino fields cannot "absorb" phases. In this case U can be cast in the form [30]

$$U = V\,P \tag{13.2}$$

where the matrix V contains the $(n-1)(n-2)/2$ Dirac CP violation phases, while P is a diagonal matrix with the additional $(n-1)$ Majorana CP violation phases α_{21}, α_{31},..., α_{n1},

$$P = diag\left(1, e^{i\frac{\alpha_{21}}{2}}, e^{i\frac{\alpha_{31}}{2}}, ..., e^{i\frac{\alpha_{n1}}{2}}\right). \tag{13.3}$$

The Majorana phases will conserve CP if [32] $\alpha_{j1} = \pi q_j$, $q_j = 0, 1, 2$, $j = 2, 3, ..., n$. In this case $\exp[i(\alpha_{j1} - \alpha_{k1})] = \pm 1$ has a simple physical interpretation: this is the relative CP-parity of Majorana neutrinos χ_j and χ_k. The condition of CP invariance of the leptonic CC weak interaction in the case of mixing and massive Majorana neutrinos reads [29]:

$$U^*_{lj} = U_{lj}\,\rho_j\,, \quad \rho_j = \frac{1}{i}\eta_{CP}(\chi_j) = \pm 1\,, \tag{13.4}$$

where $\eta_{CP}(\chi_j) = i\rho_j = \pm i$ is the CP parity of the Majorana neutrino χ_j [32]. Thus, if CP invariance holds, the elements of U are either real or purely imaginary.

In the case of $n = 3$ there are altogether 3 CP violation phases - one Dirac and two Majorana. Even in the mixing involving only 2 massive Majorana neutrinos there is one physical CP violation Majorana phase. In contrast, the CC weak interaction is automatically CP-invariant in the case of mixing of two massive Dirac neutrinos or of two quarks.

13.2. Neutrino oscillations in vacuum

Neutrino oscillations are a quantum mechanical consequence of the existence of nonzero neutrino masses and neutrino (lepton) mixing, Eq. (13.1), and of the relatively small splitting between the neutrino masses. The neutrino mixing and oscillation phenomena are analogous to the $K^0 - \bar{K}^0$ and $B^0 - \bar{B}^0$ mixing and oscillations.

In what follows we will present a simplified version of the derivation of the expressions for the neutrino and antineutrino oscillation probabilities. The complete derivation would require the use of the wave packet formalism for the evolution of the massive neutrino states, or, alternatively, of the field-theoretical approach, in which one takes into account the processes of production, propagation and detection of neutrinos [33].

Suppose the flavour neutrino ν_l is produced in a CC weak interaction process and after a time T it is observed by a neutrino detector, located at a distance L from the neutrino source and capable of detecting also neutrinos $\nu_{l'}$, $l' \neq l$. We will consider the evolution of the neutrino state $|\nu_l\rangle$ in the frame in which the detector is at rest (laboratory frame). The oscillation probability, as we will see, is a Lorentz invariant quantity. If lepton mixing, Eq. (13.1), takes place and the masses m_j of all neutrinos ν_j are sufficiently small, the state of the neutrino ν_l, $|\nu_l\rangle$, will be a coherent superposition of the states $|\nu_j\rangle$ of neutrinos ν_j:

$$|\nu_l\rangle = \sum_j U^*_{lj}\,|\nu_j; \tilde{p}_j\rangle, \quad l = e, \mu, \tau\,, \tag{13.5}$$

where U is the neutrino mixing matrix and $\tilde{p}_j$ is the 4-momentum of ν_j [34].

We will consider the case of relativistic neutrinos ν_j, which corresponds to the conditions in both past and currently planned future neutrino oscillation experiments [36]. In this case the state $|\nu_j; \tilde{p}_j\rangle$ practically coincides with the helicity (-1) state $|\nu_j, L; \tilde{p}_j\rangle$ of the neutrino ν_j, the admixture of the helicity (+1) state $|\nu_j, R; \tilde{p}_j\rangle$ in $|\nu_j; \tilde{p}_j\rangle$ being suppressed due to the factor $\sim m_j/E_j$, where E_j is the energy of ν_j. If ν_j are Majorana particles, $\nu_j \equiv \chi_j$, due to the presence of the helicity (+1) state $|\chi_j, R; \tilde{p}_j\rangle$ in $|\chi_j; \tilde{p}_j\rangle$, the neutrino ν_l can produce an l^+ (instead of l^-) when it interacts with nucleons. The cross section of such a $|\Delta L_l| = 2$ process is suppressed by the factor $(m_j/E_j)^2$, which renders the process unobservable at present.

If the number n of massive neutrinos ν_j is bigger than 3 due to a mixing between the active flavour and sterile neutrinos, one will have additional relations similar to that in Eq. (13.5) for the state vectors of the (predominantly LH) sterile antineutrinos. In the case of just one RH sterile neutrino field $\nu_{sR}(x)$, for instance, we will have in addition to Eq. (13.5):

$$|\bar{\nu}_{sL}\rangle = \sum_{j=1}^{4} U^*_{sj}\,|\nu_j; \tilde{p}_j\rangle \cong \sum_{j=1}^{4} U^*_{sj}\,|\nu_j, L; \tilde{p}_j\rangle\,, \tag{13.6}$$

where the neutrino mixing matrix U is now a 4×4 unitary matrix.

For the state vector of RH flavour antineutrino $\bar{\nu}_l$, produced in a CC weak interaction process we similarly get:

$$|\bar{\nu}_l\rangle = \sum_j U_{lj}\,|\bar{\nu}_j; \tilde{p}_j\rangle \cong \sum_{j=1} U_{lj}\,|\bar{\nu}_j, R; \tilde{p}_j\rangle, \quad l = e, \mu, \tau\,, \tag{13.7}$$

where $|\bar{\nu}_j, R; \tilde{p}_j\rangle$ is the helicity (+1) state of the antineutrino $\bar{\nu}_j$ if ν_j are Dirac fermions, or the helicity (+1) state of the neutrino $\nu_j \equiv \bar{\nu}_j \equiv \chi_j$ if the massive neutrinos are Majorana particles. Thus, in the latter case we have in Eq. (13.7): $|\bar{\nu}_j; \tilde{p}_j\rangle \cong |\nu_j, R; \tilde{p}_j\rangle \equiv |\chi_j, R; \tilde{p}_j\rangle$. The presence of the matrix U in Eq. (13.7) (and not of U^*) follows directly from Eq. (13.1).

We will assume in what follows that the spectrum of masses of neutrinos is not degenerate: $m_j \neq m_k$, $j \neq k$. Then the states $|\nu_j; \tilde{p}_j\rangle$ in the linear superposition in the r.h.s. of Eq. (13.5) will have, in general, different energies and different momenta, independently of whether they are produced in a decay or interaction process: $\tilde{p}_j \neq \tilde{p}_k$, or $E_j \neq E_k$, $\mathbf{p}_j \neq \mathbf{p}_k$, $j \neq k$, where $E_j = \sqrt{p_j^2 + m_j^2}$, $p_j \equiv |\mathbf{p}_j|$. The deviations of E_j and p_j from the values for a massless neutrino E and $p = E$ are proportional to m_j^2/E_0, E_0 being a characteristic energy of the process, and are extremely small. In the case of $\pi^+ \to \mu^+ + \nu_\mu$ decay at rest, for instance, we have: $E_j = E + m_j^2/(2m_\pi)$, $p_j = E - \xi m_j^2/(2E)$, where $E = (m_\pi/2)(1 - m_\mu^2/m_\pi^2) \cong 30$ MeV, $\xi = (1 + m_\mu^2/m_\pi^2)/2 \cong 0.8$, and m_μ and m_π are the μ^+ and π^+ masses. Taking $m_j = 1$ eV we find: $E_j \cong E\,(1 + 1.2 \times 10^{-16})$ and $p_j \cong E\,(1 - 4.4 \times 10^{-16})$.

Suppose that the neutrinos are observed via a CC weak interaction process and that in the detector's rest frame they are detected after time T after emission, after traveling a distance L. Then the amplitude of the probability that neutrino $\nu_{l'}$ will be observed if neutrino ν_l was produced by the neutrino source can be written as [33,35,37]:

$$A(\nu_l \to \nu_{l'}) = \sum_j U_{l'j}\,D_j\,U^\dagger_{jl}\,, \quad l, l' = e, \mu, \tau\,, \tag{13.8}$$

where $D_j = D_j(p_j; L, T)$ describes the propagation of ν_j between the source and the detector, $U^\dagger_{jl}$ and $U_{l'j}$ are the amplitudes to find ν_j in the initial and in the final flavour neutrino state, respectively. It follows from relativistic Quantum Mechanics considerations that [33,35]

$$D_j \equiv D_j(\tilde{p}_j; L, T) = e^{-i\tilde{p}_j\,(x_f - x_0)} = e^{-i(E_j T - p_j L)}\,, \qquad p_j \equiv |\mathbf{p}_j|\,, \tag{13.9}$$

where [38] x_0 and x_f are the space-time coordinates of the points of neutrino production and detection, $T = (t_f - t_0)$ and $L = \mathbf{k}(\mathbf{x}_f - \mathbf{x}_0)$, $\mathbf{k}$ being the unit vector in the direction of neutrino momentum,

$\mathbf{p}_j = \mathbf{k}\mathrm{p_j}$. What is relevant for the calculation of the probability $P(\nu_l \to \nu_{l'}) = |A(\nu_l \to \nu_{l'})|^2$ is the interference factor $D_j D_k^*$ which depends on the phase

$$\delta\varphi_{jk} = (E_j - E_k)T - (p_j - p_k)L = (E_j - E_k)\left[T - \frac{E_j + E_k}{p_j + p_k}\,L\right] + \frac{m_j^2 - m_k^2}{p_j + p_k}\,L\,. \tag{13.10}$$

Some authors [39] have suggested that the distance traveled by the neutrinos L and the time interval T are related by $T = (E_j+E_k)\,L/(p_j+p_k) = L/\bar{v}$, $\bar{v} = (E_j/(E_j+E_k))v_j + (E_k/(E_j+E_k))v_k$ being the "average" velocity of ν_j and ν_k, where $v_{j,k} = p_{j,k}/E_{j,k}$. In this case the first term in the r.h.s. of Eq. (13.10) vanishes. The indicated relation has not emerged so far from any dynamical wave packet calculations. We arrive at the same conclusion concerning the term under discussion in Eq. (13.10) if one assumes [40] that $E_j = E_k = E_0$. Finally, it was proposed in Ref. 37 and Ref. 41 that the states of ν_j and $\bar{\nu}_j$ in Eq. (13.5) and Eq. (13.7) have the same 3-momentum, $p_j = p_k = p$. Under this condition the first term in the r.h.s. of Eq. (13.10) is negligible, being suppressed by the additional factor $(m_j^2 + m_k^2)/p^2$ since for relativistic neutrinos $L = T$ up to terms $\sim m_{j,k}^2/p^2$. We arrive at the same conclusion if $E_j \neq E_k$, $p_j \neq p_k$, $j \neq k$, and we take into account that neutrinos are relativistic and therefore, up to corrections $\sim m_{j,k}^2/E_{j,k}^2$, we have $L \cong T$ (see, *e.g.*, C. Giunti quoted in Ref. 33).

Although the cases considered above are physically quite different, they lead to the same result for the phase difference $\delta\varphi_{jk}$. Thus, we have:

$$\delta\varphi_{jk} \cong \frac{m_j^2 - m_k^2}{2p}\,L = 2\pi\,\frac{L}{L_{jk}^v}\,\mathrm{sgn}(m_j^2 - m_k^2)\,, \tag{13.11}$$

where $p = (p_j + p_k)/2$ and

$$L_{jk}^v = 4\pi\frac{p}{|\Delta m_{jk}^2|} \cong 2.48\ \mathrm{m}\ \frac{p[MeV]}{|\Delta m_{jk}^2|[eV^2]} \tag{13.12}$$

is the neutrino oscillation length associated with Δm_{jk}^2. We can safely neglect the dependence of p_j and p_k on the masses m_j and m_k and consider p to be the zero neutrino mass momentum, $p = E$. The phase difference $\delta\varphi_{jk}$, Eq. (13.11), is Lorentz-invariant.

Eq. (13.9) corresponds to a plane-wave description of the propagation of neutrinos ν_j. It accounts only for the movement of the center of the wave packet describing ν_j. In the wave packet treatment of the problem, the interference between the states of ν_j and ν_k is subject to a number of conditions [33], the localisation condition and the condition of overlapping of the wave packets of ν_j and ν_k at the detection point being the most important. For relativistic neutrinos, the localisation condition reads: $\sigma_{xP}, \sigma_{xD} < L_{jk}^v/(2\pi)$, $\sigma_{xP(D)}$ being the spatial width of the production (detection) wave packet. Thus, the interference will not be suppressed if the spatial width of the neutrino wave packets detetermined by the neutrino production and detection processes is smaller than the corresponding oscillation length in vacuum. In order for the interference to be nonzero, the wave packets describing ν_j and ν_k should also overlap in the point of neutrino detection. This requires that the spatial separation between the two wave packets at the point of neutrinos detection, caused by the two wave packets having different group velocities $v_j \neq v_k$, satisfies $|(v_j - v_k)T| \ll \max(\sigma_{xP}, \sigma_{xD})$. If the interval of time T is not measured, T in the preceding condition must be replaced by the distance L between the neutrino source and the detector (for further discussion see, *e.g.*, [33,35,37]) .

For the $\nu_l \to \nu_{l'}$ and $\bar{\nu}_l \to \bar{\nu}_{l'}$ oscillation probabilities we get from Eq. (13.8), Eq. (13.9), and Eq. (13.11):

$$P(\nu_l \to \nu_{l'}) = \sum_j |U_{l'j}|^2\,|U_{lj}|^2 + 2\sum_{j>k} |U_{l'j}\,U_{lj}^*\,U_{lk}\,U_{l'k}^*| \cos\left(\frac{\Delta m_{jk}^2}{2p}\,L - \phi_{l'l;jk}\right), \tag{13.13}$$

$$P(\bar{\nu}_l \to \bar{\nu}_{l'}) = \sum_j |U_{l'j}|^2\,|U_{lj}|^2 + 2\sum_{j>k} |U_{l'j}\,U_{lj}^*\,U_{lk}\,U_{l'k}^*| \cos\left(\frac{\Delta m_{jk}^2}{2p}\,L + \phi_{l'l;jk}\right), \tag{13.14}$$

where $l, l' = e, \mu, \tau$ and $\phi_{l'l;jk} = \arg\left(U_{l'j}\,U_{lj}^*\,U_{lk}\,U_{l'k}^*\right)$. It follows from Eq. (13.8) - Eq. (13.10) that in order for neutrino oscillations to occur, at least two neutrinos ν_j should not be degenerate in mass and lepton mixing should take place, $U \neq \mathbf{1}$. The neutrino oscillations effects can be large if we have

$$\frac{|\Delta m_{jk}^2|}{2p}\,L = 2\pi\,\frac{L}{L_{jk}^v} \gtrsim 1\,,\ \ j \neq k\,. \tag{13.15}$$

at least for one Δm_{jk}^2. This condition has a simple physical interpretation: the neutrino oscillation length L_{jk}^v should be of the order of, or smaller, than source-detector distance L, otherwise the oscillations will not have time to develop before neutrinos reach the detector.

We see from Eq. (13.13) and Eq. (13.14) that $P(\nu_l \to \nu_{l'}) = P(\bar{\nu}_{l'} \to \bar{\nu}_l)$, $l, l' = e, \mu, \tau$. This is a consequence of CPT invariance. The conditions of CP and T invariance read [30,42,43]: $P(\nu_l \to \nu_{l'}) = P(\bar{\nu}_l \to \bar{\nu}_{l'})$, $l, l' = e, \mu, \tau$ (CP), $P(\nu_l \to \nu_{l'}) = P(\nu_{l'} \to \nu_l)$, $P(\bar{\nu}_l \to \bar{\nu}_{l'}) = P(\bar{\nu}_{l'} \to \bar{\nu}_l)$, $l, l' = e, \mu, \tau$ (T). In the case of CPT invariance, which we will assume to hold throughout this article, we get for the survival probabilities: $P(\nu_l \to \nu_l) = P(\bar{\nu}_l \to \bar{\nu}_l)$, $l, l' = e, \mu, \tau$. Thus, the study of the "disappearance" of ν_l and $\bar{\nu}_l$, caused by oscillations in vacuum, cannot be used to test whether CP invariance holds in the lepton sector. It follows from Eq. (13.13) and Eq. (13.14) that we can have CP violation effects in neutrino oscillations only if $\phi_{l'l;jk} \neq \pi q$, $q = 0, 1, 2$, *i.e.*, if $U_{l'j}\,U_{lj}^*\,U_{lk}\,U_{l'k}^*$, and therefore U itself, is not real. As a measure of CP and T violation in neutrino oscillations we can consider the asymmetries:

$$A_{\mathrm{CP}}^{(l'l)} \equiv P(\nu_l \to \nu_{l'}) - P(\bar{\nu}_l \to \bar{\nu}_{l'})\,, \quad A_{\mathrm{T}}^{(l'l)} \equiv P(\nu_l \to \nu_{l'}) - P(\nu_{l'} \to \nu_l)\,. \tag{13.16}$$

CPT invariance implies: $A_{\mathrm{CP}}^{(l'l)} = -A_{\mathrm{CP}}^{(ll')}$, $A_{\mathrm{T}}^{(l'l)} = P(\bar{\nu}_{l'} \to \bar{\nu}_l) - P(\bar{\nu}_l \to \bar{\nu}_{l'}) = A_{\mathrm{CP}}^{(l'l)}$. It follows further directly from Eq. (13.13) and Eq. (13.14) that

$$A_{\mathrm{CP}}^{(l'l)} = 4\sum_{j>k} \mathrm{Im}\left(U_{l'j}\,U_{lj}^*\,U_{lk}\,U_{l'k}^*\right) \sin\frac{\Delta m_{jk}^2}{2p}\,L\,,\ \ l, l' = e, \mu, \tau\,. \tag{13.17}$$

Eq. (13.2) and Eq. (13.13) - Eq. (13.14) imply that $P(\nu_l \to \nu_{l'})$ and $P(\bar{\nu}_l \to \bar{\nu}_{l'})$ do not depend on the Majorana CP violation phases in the neutrino mixing matrix U [30]. Thus, the experiments investigating the $\nu_l \to \nu_{l'}$ and $\bar{\nu}_l \to \bar{\nu}_{l'}$ oscillations, $l, l' = e, \mu, \tau$, cannot provide information on the nature - Dirac or Majorana, of massive neutrinos. The same conclusions hold also when the $\nu_l \to \nu_{l'}$ and $\bar{\nu}_l \to \bar{\nu}_{l'}$ oscillations take place in matter [44]. In the case of $\nu_l \leftrightarrow \nu_{l'}$ and $\bar{\nu}_l \leftrightarrow \bar{\nu}_{l'}$ oscillations in vacuum, only the Dirac phase(s) in U can cause CP violating effects leading to $P(\nu_l \to \nu_{l'}) \neq P(\bar{\nu}_l \to \bar{\nu}_{l'})$, $l \neq l'$.

In the case of 3-neutrino mixing all different $\mathrm{Im}(U_{l'j}U_{lj}^*U_{lk}U_{l'k}^*)$ coincide up to a sign as a consequence of the unitarity of U. Therefore one has [45]:

$$A_{\mathrm{CP}}^{(\mu e)} = -A_{\mathrm{CP}}^{(\tau e)} = A_{\mathrm{CP}}^{(\tau\mu)} = 4\,J_{\mathrm{CP}}\,\left(\sin\frac{\Delta m_{32}^2}{2p}\,L + \sin\frac{\Delta m_{21}^2}{2p}\,L + \sin\frac{\Delta m_{13}^2}{2p}\,L\right) \tag{13.18}$$

where

$$J_{\mathrm{CP}} = \mathrm{Im}\left(U_{\mu 3}\,U_{e3}^*\,U_{e2}\,U_{\mu 2}^*\right)\,, \tag{13.19}$$

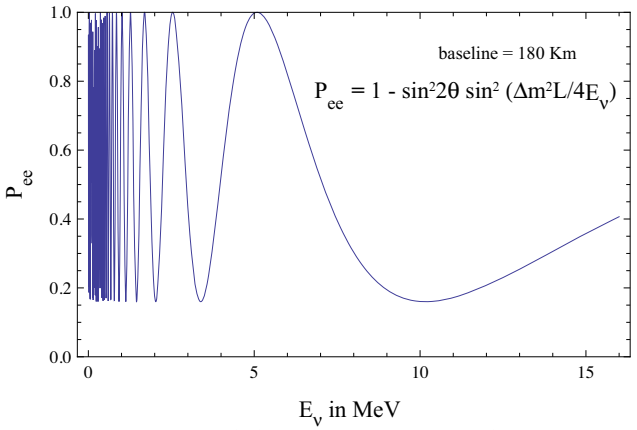

Figure 13.1: The ν_e ($\bar{\nu}_e$) survival probability $P(\nu_e \to \nu_e) = P(\bar{\nu}_e \to \bar{\nu}_e)$, Eq. (13.30), as a function of the neutrino energy for $L = 180$ km, $\Delta m^2 = 7.0 \times 10^{-5}$ eV^2 and $\sin^2 2\theta = 0.84$ (from [48]) .

is the "rephasing invariant" associated with the Dirac CP violation phase in U. It is analogous to the rephasing invariant associated with the Dirac CP violating phase in the CKM quark mixing matrix [46]. It is clear from Eq. (13.18) that $J_{\rm CP}$ controls the magnitude of CP violation effects in neutrino oscillations in the case of 3-neutrino mixing. If $\sin(\Delta m^2_{ij}/(2p))L \cong 0$ for $(ij) = (32)$, or (21), or (13), we get $A^{(l'l)}_{\rm CP} \cong 0$. Thus, if as a consequence of the production, propagation and/or detection of neutrinos, effectively oscillations due only to one non-zero neutrino mass squared difference take place, the CP violating effects will be strongly suppressed. In particular, we get $A^{(l'l)}_{\rm CP} = 0$, unless all three $\Delta m^2_{ij} \neq 0$, $(ij) = (32), (21), (13)$.

If the number of massive neutrinos n is equal to the number of neutrino flavours, $n = 3$, one has as a consequence of the unitarity of the neutrino mixing matrix: $\sum_{l'=e,\mu,\tau} P(\nu_l \to \nu_{l'}) = 1$, $l = e, \mu, \tau$, $\sum_{l=e,\mu,\tau} P(\nu_l \to \nu_{l'}) = 1$, $l' = e, \mu, \tau$. Similar "probability conservation" equations hold for $P(\bar{\nu}_l \to \bar{\nu}_{l'})$. If, however, the number of light massive neutrinos is bigger than the number of flavour neutrinos as a consequence, *e.g.*, of a flavour neutrino - sterile neutrino mixing, we would have $\sum_{l'=e,\mu,\tau} P(\nu_l \to \nu_{l'}) = 1 - P(\nu_l \to \bar{\nu}_{sL})$, $l = e, \mu, \tau$, where we have assumed the existence of just one sterile neutrino. Obviously, in this case $\sum_{l'=e,\mu,\tau} P(\nu_l \to \nu_{l'}) < 1$ if $P(\nu_l \to \bar{\nu}_{sL}) \neq 0$. The former inequality is used in the searches for oscillations between active and sterile neutrinos.

Consider next neutrino oscillations in the case of one neutrino mass squared difference "dominance": suppose that $|\Delta m^2_{j1}| \ll |\Delta m^2_{n1}|$, $j = 2, ..., (n-1)$, $|\Delta m^2_{n1}|\, L/(2p) \gtrsim 1$ and $|\Delta m^2_{j1}|\, L/(2p) \ll 1$, so that $\exp[i(\Delta m^2_{j1}\, L/(2p)] \cong 1$, $j = 2, ..., (n-1)$. Under these conditions we obtain from Eq. (13.13) and Eq. (13.14), keeping only the oscillating terms involving Δm^2_{n1}:

$$P(\nu_{l(l')} \to \nu_{l'(l)}) \cong P(\bar{\nu}_{l(l')} \to \bar{\nu}_{l'(l)}) \cong \delta_{ll'} - 2|U_{ln}|^2 \left[\delta_{ll'} - |U_{l'n}|^2\right] \left(1 - \cos\frac{\Delta m^2_{n1}}{2p}\, L\right). \tag{13.20}$$

It follows from the neutrino oscillation data (Sections 13.4 and 13.5) that in the case of 3-neutrino mixing, one of the two independent neutrino mass squared differences, say Δm^2_{21}, is much smaller in absolute value than the second one, Δm^2_{31}: $|\Delta m^2_{21}| \ll |\Delta m^2_{31}|$. The data imply:

$$\begin{aligned} |\Delta m^2_{21}| &\cong 7.6 \times 10^{-5}\ \text{eV}^2\,, \\ |\Delta m^2_{31}| &\cong 2.4 \times 10^{-3}\ \text{eV}^2\,, \\ |\Delta m^2_{21}|/|\Delta m^2_{31}| &\cong 0.032\,. \end{aligned} \tag{13.21}$$

Neglecting the effects due to Δm^2_{21} we get from Eq. (13.20) by setting $n = 3$ and choosing, *e.g.*, i) $l = l' = e$ and ii) $l = e(\mu)$, $l' = \mu(e)$ [47]:

$$P(\nu_e \to \nu_e) = P(\bar{\nu}_e \to \bar{\nu}_e) \cong 1 - 2|U_{e3}|^2 \left(1 - |U_{e3}|^2\right) \left(1 - \cos\frac{\Delta m^2_{31}}{2p}\, L\right), \tag{13.22}$$

$$\begin{aligned} P(\nu_{\mu(e)} \to \nu_{e(\mu)}) &\cong 2\,|U_{\mu 3}|^2\,|U_{e3}|^2 \left(1 - \cos\frac{\Delta m^2_{31}}{2p}\, L\right) \\ &= \frac{|U_{\mu 3}|^2}{1 - |U_{e3}|^2}\, P^{2\nu}\left(|U_{e3}|^2, m^2_{31}\right), \end{aligned} \tag{13.23}$$

and $P(\bar{\nu}_{\mu(e)} \to \bar{\nu}_{e(\mu)}) = P(\nu_{\mu(e)} \to \nu_{e(\mu)})$. Here $P^{2\nu}\left(|U_{e3}|^2, m^2_{31}\right)$ is the probability of the 2-neutrino transition $\nu_e \to (s_{23}\nu_\mu + c_{23}\nu_\tau)$ due to Δm^2_{31} and a mixing with angle θ_{13}, where

$$\sin^2\theta_{13} = |U_{e3}|^2\,,\ \ s^2_{23} \equiv \sin^2\theta_{23} = \frac{|U_{\mu 3}|^2}{1 - |U_{e3}|^2}\,,\ \ c^2_{23} \equiv \cos^2\theta_{23} = \frac{|U_{\tau 3}|^2}{1 - |U_{e3}|^2} \tag{13.24}$$

Table 13.1: Sensitivity of different oscillation experiments.

Source	Type of ν	$\overline{E}$[MeV]	L[km]	min(Δm^2)[eV^2]
Reactor	$\overline{\nu}_e$	~ 1	1	$\sim 10^{-3}$
Reactor	$\overline{\nu}_e$	~ 1	100	$\sim 10^{-5}$
Accelerator	$\nu_\mu, \overline{\nu}_\mu$	$\sim 10^3$	1	~ 1
Accelerator	$\nu_\mu, \overline{\nu}_\mu$	$\sim 10^3$	1000	$\sim 10^{-3}$
Atmospheric ν's	$\nu_{\mu,e}, \overline{\nu}_{\mu,e}$	$\sim 10^3$	10^4	$\sim 10^{-4}$
Sun	ν_e	~ 1	1.5×10^8	$\sim 10^{11}$

Eq. (13.22) describes with a relatively high precision the oscillations of reactor $\bar{\nu}_e$ on a distance $L \sim 1$ km in the case of 3-neutrino mixing. It was used in the analysis of the results of the CHOOZ experiment and can be used in the analyses of the data of the Double Chooz, Daya Bay and RENO experiments, which are under preparation. Eq. (13.20) with $n = 3$ and $l = l' = \mu$ describes with a relatively good precision the effects of oscillations of the accelerator ν_μ, seen in the K2K and MINOS experiments. The $\nu_\mu \to \nu_\tau$ oscillations, which the OPERA experiment is aiming to detect, can be described by Eq. (13.20) with $n = 3$ and $l = \mu$, $l' = \tau$. Finally, the probability Eq. (13.23) describes with a good precision the $\nu_\mu \to \nu_e$ and $\bar{\nu}_\mu \to \bar{\nu}_e$ oscillations under the conditions of the MINOS experiment.

In certain cases the dimensions of the neutrino source, ΔL, are not negligible in comparison with the oscillation length. Similarly, when analyzing neutrino oscillation data one has to include the energy resolution of the detector, ΔE, *etc.* in the analysis. As can be shown [29], if $2\pi\Delta L/L^v_{jk} \gg 1$, and/or $2\pi(L/L^v_{jk})(\Delta E/E) \gg 1$, the oscillating terms in the neutrino oscillation probabilities will be strongly suppressed. In this case (as well as in the case of sufficiently large separation of the ν_j and ν_k wave packets at the detection point) the interference terms in $P(\nu_l \to \nu_{l'})$ and $P(\bar{\nu}_{l'} \to \bar{\nu}_l)$ will be negligibly small and the neutrino flavour conversion will be determined by the average probabilities:

$$\bar{P}(\nu_l \to \nu_{l'}) = \bar{P}(\bar{\nu}_l \to \bar{\nu}_{l'}) \cong \sum_j |U_{l'j}|^2\,|U_{lj}|^2\,. \tag{13.25}$$

Suppose next that in the case of 3-neutrino mixing, $|\Delta m^2_{21}|\, L/(2p) \sim 1$, while at the same time $|\Delta m^2_{31(32)}|\, L/(2p) \gg 1$, and the oscillations due to Δm^2_{31} and Δm^2_{32} are strongly suppressed (averaged out) due to integration over the region of neutrino production, the energy resolution function, *etc.* In this case we get for the ν_e and $\bar{\nu}_e$ survival probabilities:

$$P(\nu_e \to \nu_e) = P(\bar{\nu}_e \to \bar{\nu}_e) \cong |U_{e3}|^4 + \left(1 - |U_{e3}|^2\right)^2\, P^{2\nu}(\nu_e \to \nu_e)\,, \tag{13.26}$$

$$P^{2\nu}(\nu_e \to \nu_e) = P^{2\nu}(\bar\nu_e \to \bar\nu_e) \equiv P^{2\nu}_{ee}(\theta_{12}, \Delta m^2_{21}) = 1 - \frac{1}{2}\sin^2 2\theta_{12}\left(1 - \cos\frac{\Delta m^2_{21}}{2p}\,L\right) \quad (13.27)$$

being the ν_e and $\bar\nu_e$ survival probability in the case of 2-neutrino oscillations "driven" by the angle θ_{12} and Δm^2_{21}, with θ_{12} determined by

$$\cos^2\theta_{12} = \frac{|U_{e1}|^2}{1-|U_{e3}|^2}\,, \quad \sin^2\theta_{12} = \frac{|U_{e2}|^2}{1-|U_{e3}|^2}\,. \quad (13.28)$$

Eq. (13.26) with $P^{2\nu}(\bar\nu_e \to \bar\nu_e)$ given by Eq. (13.27) describes the effects of neutrino oscillations of reactor $\bar\nu_e$ observed by the KamLAND experiment.

In the case of 3-neutrino mixing with $0 < \Delta m^2_{21} < |\Delta m^2_{31(32)}|$ and $|U_{e3}|^2 = |\sin\theta_{13}|^2 \ll 1$ (see Section 13.6), one can identify Δm^2_{21} and θ_{12} as the neutrino mass squared difference and mixing angle responsible for the solar ν_e oscillations, and Δm^2_{31} and θ_{23} as those associated with the dominant atmospheric ν_μ and $\bar\nu_\mu$ oscillations. Thus, θ_{12} and θ_{23} are often called "solar" and "atmospheric" neutrino mixing angles and denoted as $\theta_{12} = \theta_\odot$ and $\theta_{23} = \theta_{\rm A}$ (or $\theta_{\rm atm}$), while Δm^2_{21} and Δm^2_{31} are often referred to as the "solar" and "atmospheric" neutrino mass squared differences and denoted as $\Delta m^2_{21} \equiv \Delta m^2_\odot$ and $\Delta m^2_{31} \equiv \Delta m^2_{\rm A}$(or $\Delta m^2_{\rm atm}$).

The data of ν-oscillations experiments is often analyzed assuming 2-neutrino mixing:

$$|\nu_l\rangle = |\nu_1\rangle\cos\theta + |\nu_2\rangle\sin\theta\,, \quad |\nu_x\rangle = -|\nu_1\rangle\sin\theta + |\nu_2\rangle\cos\theta\,, \quad (13.29)$$

where θ is the neutrino mixing angle in vacuum and ν_x is another flavour neutrino or sterile (anti-) neutrino, $x = l' \neq l$ or $\nu_x \equiv \bar\nu_{sL}$. In this case we have [41]:

$$P^{2\nu}(\nu_l \to \nu_l) = 1 - \frac{1}{2}\sin^2 2\theta\left(1 - \cos 2\pi\frac{L}{L^v}\right),$$
$$P^{2\nu}(\nu_l \to \nu_x) = 1 - P^{2\nu}(\nu_l \to \nu_l)\,, \quad (13.30)$$

where $L^v = 4\pi\,p/\Delta m^2$, $\Delta m^2 = m^2_2 - m^2_1 > 0$. Combining the CPT invariance constraints with the probability conservation one obtains: $P(\nu_l \to \nu_x) = P(\bar\nu_l \to \bar\nu_x) = P(\nu_x \to \nu_l) = P(\bar\nu_x \to \bar\nu_l)$. These equalities and Eq. (13.30) with $l = \mu$ and $x = \tau$ were used, for instance, in the analysis of the Super-K atmospheric neutrino data [13], in which the first compelling evidence for oscillations of neutrinos was obtained. The probability $P^{2\nu}(\nu_l \to \nu_x)$, Eq. (13.30), depends on two factors: on $(1-\cos 2\pi L/L^v)$, which exhibits oscillatory dependence on the distance L and on the neutrino energy $p = E$ (hence the name "neutrino oscillations"), and on $\sin^2 2\theta$, which determines the amplitude of the oscillations. In order to have $P^{2\nu}(\nu_l \to \nu_x) \cong 1$, two conditions have to be fulfilled: one should have $\sin^2 2\theta \cong 1$ and $L^v \lesssim 2\pi L$ with $\cos 2\pi L/L^v \cong -1$. If $L^v \gg 2\pi L$, the oscillations do not have enough time to develop on the way to the neutrino detector and $P(\nu_l \to \nu_x) \cong 0$. This is illustrated in Fig. 1 showing the dependence of the probability $P^{2\nu}(\nu_e \to \nu_e) = P^{2\nu}(\bar\nu_e \to \bar\nu_e)$ on the neutrino energy.

A given experiment searching for neutrino oscillations is specified, in particular, by the average energy of the neutrinos being studied, $\bar E$, and by the source-detector distance L. The requirement $L^v_{jk} \lesssim 2\pi L$ determines the minimal value of a generic neutrino mass squared difference $\Delta m^2 > 0$, to which the experiment is sensitive (figure of merit of the experiment): $\min(\Delta m^2) \sim 2\bar E/L$. Because of the interference nature of neutrino oscillations, experiments can probe, in general, rather small values of Δm^2 (see, *e.g.*, Ref. 37). Values of $\min(\Delta m^2)$, characterizing qualitatively the sensitivity of different experiments are given in Table 1. They correspond to the reactor experiments CHOOZ ($L \sim 1$ km) and KamLAND ($L \sim 100$ km), to accelerator experiments - past ($L \sim 1$ km), recent, current and future (K2K, MINOS, OPERA, T2K, NOνA), $L \sim (300 \div 1000)$ km), to the Super-Kamiokande experiment studying atmospheric neutrino oscillations, and to the solar neutrino experiments.

13.3. Matter effects in neutrino oscillations

The presence of matter can change drastically the pattern of neutrino oscillations: neutrinos can interact with the particles forming the matter. Accordingly, the Hamiltonian of the neutrino system in matter H_m, differs from the Hamiltonian in vacuum H_0, $H_m = H_0 + H_{int}$, where H_{int} describes the interaction of neutrinos with the particles of matter. When, for instance, ν_e and ν_μ propagate in matter, they can scatter (due to H_{int}) on the electrons (e^-), protons (p) and neutrons (n) present in matter. The incoherent elastic and the quasi-elastic scattering, in which the states of the initial particles change in the process (destroying the coherence between the neutrino states), are not of interest - they have a negligible effect on the solar neutrino propagation in the Sun and on the solar, atmospheric and reactor neutrino propagation in the Earth [49]: even in the center of the Sun, where the matter density is relatively high (~ 150 g/cm^3), a ν_e with energy of 1 MeV has a mean free path with respect to the indicated scattering processes $\sim 10^{10}$ km. We recall that the solar radius is much smaller: $\rm R_\odot = 6.96 \times 10^5$ km. The oscillating ν_e and ν_μ can scatter also elastically in the forward direction on the e^-, p and n, with the momenta and the spin states of the particles remaining unchanged. In such a process the coherence of the neutrino states is preserved.

The ν_e and ν_μ coherent elastic scattering on the particles of matter generates nontrivial indices of refraction of the ν_e and ν_μ in matter [25]: $\kappa(\nu_e) \neq 1$, $\kappa(\nu_\mu) \neq 1$. Most importantly, we have $\kappa(\nu_e) \neq \kappa(\nu_\mu)$. The difference $\kappa(\nu_e) - \kappa(\nu_\mu)$ is determined essentially by the difference of the real parts of the forward $\nu_e - e^-$ and $\nu_\mu - e^-$ elastic scattering amplitudes [25] Re $[\rm F_{\nu_e - e^-}(0)]$ − Re $[\rm F_{\nu_\mu - e^-}(0)]$: due to the flavour symmetry of the neutrino – quark (neutrino – nucleon) neutral current interaction, the forward $\nu_e - p, n$ and $\nu_\mu - p, n$ elastic scattering amplitudes are equal and therefore do not contribute to the difference of interest [50]. The imaginary parts of the forward scattering amplitudes (responsible, in particular, for decoherence effects) are proportional to the corresponding total scattering cross-sections and in the case of interest are negligible in comparison with the real parts. The real parts of the amplitudes $\rm F_{\nu_e - e^-}(0)$ and $\rm F_{\nu_\mu - e^-}(0)$ can be calculated in the Standard Model. To leading order in the Fermi constant G_F, only the term in $\rm F_{\nu_e - e^-}(0)$ due to the diagram with exchange of a virtual $W^\pm$-boson contributes to $\rm F_{\nu_e - e^-}(0) - F_{\nu_\mu - e^-}(0)$. One finds the following result for $\kappa(\nu_e) - \kappa(\nu_\mu)$ in the rest frame of the scatters [25,52,53]:

$$\kappa(\nu_e) - \kappa(\nu_\mu) = \frac{2\pi}{p^2}\left(\text{Re }[\rm F_{\nu_e - e^-}(0)] - \text{Re }[\rm F_{\nu_\mu - e^-}(0)]\right) = -\frac{1}{p}\sqrt{2}G_F N_e\,, \quad (13.31)$$

where N_e is the electron number density in matter. Given $\kappa(\nu_e) - \kappa(\nu_\mu)$, the system of evolution equations describing the $\nu_e \leftrightarrow \nu_\mu$ oscillations in matter reads [25]:

$$i\frac{d}{dt}\begin{pmatrix} A_e(t,t_0) \\ A_\mu(t,t_0)\end{pmatrix} = \begin{pmatrix} -\epsilon(t) & \epsilon' \\ \epsilon' & \epsilon(t)\end{pmatrix}\begin{pmatrix} A_e(t,t_0) \\ A_\mu(t,t_0)\end{pmatrix} \quad (13.32)$$

where $A_e(t,t_0)$ ($A_\mu(t,t_0)$) is the amplitude of the probability to find ν_e (ν_μ) at time t of the evolution of the system if at time $t_0 \leq t$ the neutrino ν_e or ν_μ has been produced and

$$\epsilon(t) = \frac{1}{2}\,[\frac{\Delta m^2}{2E}\cos 2\theta - \sqrt{2}G_F N_e(t)], \;\; \epsilon' = \frac{\Delta m^2}{4E}\sin 2\theta. \quad (13.33)$$

The term $\sqrt{2}G_F N_e(t)$ in $\epsilon(t)$ accounts for the effects of matter on neutrino oscillations. The system of evolution equations describing the oscillations of antineutrinos $\bar\nu_e \leftrightarrow \bar\nu_\mu$ in matter has exactly the same form except for the matter term in $\epsilon(t)$ which changes sign. The effect of matter in neutrino oscillations is usually called the Mikheyev, Smirnov, Wolfenstein (or MSW) effect.

Consider first the case of $\nu_e \leftrightarrow \nu_\mu$ oscillations in matter with constant density: $N_e(t) = N_e = const$. Due to the interaction term H_{int} in H_m, the eigenstates of the Hamiltonian of the neutrino system

in vacuum, $|\nu_{1,2}\rangle$ are not eigenstates of H_m. For the eigenstates $|\nu^m_{1,2}\rangle$ of H_m, which diagonalize the evolution matrix in the r.h.s. of the system Eq. (13.32) we have:

$$|\nu_e\rangle = |\nu^m_1\rangle \cos\theta_m + |\nu^m_2\rangle \sin\theta_m\,, \qquad |\nu_\mu\rangle = -|\nu^m_1\rangle \sin\theta_m\ + |\nu^m_2\rangle \cos\theta_m\ . \tag{13.34}$$

Here θ_m is the neutrino mixing angle in matter [25],

$$\sin 2\theta_m = \frac{\tan 2\theta}{\sqrt{(1-\frac{N_e}{N^{res}_e})^2 + \tan^2 2\theta}},\ \cos 2\theta_m = \frac{1 - N_e/N^{res}_e}{\sqrt{(1-\frac{N_e}{N^{res}_e})^2 + \tan^2 2\theta}}, \tag{13.35}$$

where the quantity

$$N^{res}_e = \frac{\Delta m^2 \cos 2\theta}{2E\sqrt{2}G_F} \cong 6.56\times 10^6\ \frac{\Delta m^2[\mathrm{eV}^2]}{E[\mathrm{MeV}]}\ \cos 2\theta\,\mathrm{cm}^{-3}\ \ \mathrm{N_A}\,, \tag{13.36}$$

is called (for $\Delta m^2 \cos 2\theta > 0$) "resonance density" [26,52], $\mathrm{N_A}$ being Avogadro's number. The "adiabatic" states $|\nu^m_{1,2}\rangle$ have energies $E^m_{1,2}$ whose difference is given by

$$E^m_2 - E^m_1 = \frac{\Delta m^2}{2E}\ \ \left((1-\frac{N_e}{N^{res}_e})^2\cos^2 2\theta + \sin^2 2\theta\right)^{\frac{1}{2}} \equiv \frac{\Delta M^2}{2E}\,. \tag{13.37}$$

The probability of $\nu_e \to \nu_\mu$ transition in matter with $N_e = const.$ has the form [52]

$$P^{2\nu}_m(\nu_e \to \nu_\mu) = |A_\mu(t)|^2 = \frac{1}{2}\sin^2 2\theta_m\ \ [1 - \cos 2\pi \frac{L}{L_m}\ ]$$
$$L_m = 2\pi/(E^m_2 - E^m_1)\,, \tag{13.38}$$

where L_m is the oscillation length in matter. As Eq. (13.35) indicates, the dependence of $\sin^2 2\theta_m$ on N_e has a resonance character [26]. Indeed, if $\Delta m^2 \cos 2\theta > 0$, for any $\sin^2 2\theta \neq 0$ there exists a value of N_e given by N^{res}_e, such that when $N_e = N^{res}_e$ we have $\sin^2 2\theta_m = 1$ independently of the value of $\sin^2 2\theta < 1$. This implies that the presence of matter can lead to a strong enhancement of the oscillation probability $P^{2\nu}_m(\nu_e \to \nu_\mu)$ even when the $\nu_e \leftrightarrow \nu_\mu$ oscillations in vacuum are suppressed due to a small value of $\sin^2 2\theta$. For obvious reasons

$$N_e = N^{res}_e \equiv \frac{\Delta m^2 \cos 2\theta}{2E\sqrt{2}G_F}\,, \tag{13.39}$$

is called the "resonance condition" [26,52], while the energy at which Eq. (13.39) holds for given N_e and $\Delta m^2 \cos 2\theta$, is referred to as the "resonance energy", E^{res}. The oscillation length at resonance is given by [26] $L^{res}_m = L^v/\sin 2\theta$, while the width in N_e of the resonance at half height reads $\Delta N^{res}_e = 2N^{res}_e \tan 2\theta$. Thus, if the mixing angle in vacuum is small, the resonance is narrow, $\Delta N^{res}_e \ll N^{res}_e$, and $L^{res}_m \gg L^v$. The energy difference $E^m_2 - E^m_1$ has a minimum at the resonance: $(E^m_2 - E^m_1)^{res} = \min\ (E^m_2 - E^m_1) = (\Delta m^2/(2E))\sin 2\theta$.

It is instructive to consider two limiting cases. If $N_e \ll N^{res}_e$, we have from Eq. (13.35) and Eq. (13.37), $\theta_m \cong \theta$, $\mathrm{L_m} \cong \mathrm{L^v}$ and neutrinos oscillate practically as in vacuum. In the limit $N_e \gg N^{res}_e$, $N^{res}_e \tan^2 2\theta$, one finds $\theta_m \cong \pi/2$ ($\cos 2\theta_m \cong -1$) and the presence of matter suppresses the $\nu_e \leftrightarrow \nu_\mu$ oscillations. In this case $|\nu_e\rangle \cong |\nu^m_2\rangle$, $|\nu_\mu\rangle = -|\nu^m_1\rangle$, *i.e.*, ν_e practically coincides with the heavier matter-eigenstate, while ν_μ coincides with the lighter one.

Since the neutral current weak interaction of neutrinos in the Standard Model is flavour symmetric, the formulae and results we have obtained are valid for the case of $\nu_e - \nu_\tau$ mixing and $\nu_e \leftrightarrow \nu_\tau$ oscillations in matter as well. The case of $\nu_\mu - \nu_\tau$ mixing, however, is different: to a relatively good precision we have [54] $\kappa(\nu_\mu) \cong \kappa(\nu_\tau)$ and the $\nu_\mu \leftrightarrow \nu_\tau$ oscillations in the matter of the Earth and the Sun proceed practically as in vacuum [55].

The analogs of Eq. (13.35) to Eq. (13.38) for oscillations of antineutrinos, $\bar\nu_e \leftrightarrow \bar\nu_\mu$, in matter can formally be obtained by replacing N_e with $(-N_e)$ in the indicated equations. It should be clear that depending on the sign of $\Delta m^2 \cos 2\theta$, the presence of matter can lead to resonance enhancement either of the $\nu_e \leftrightarrow \nu_\mu$ or of the $\bar\nu_e \leftrightarrow \bar\nu_\mu$ oscillations, but not of both types of oscillations [52]. For $\Delta m^2 \cos 2\theta < 0$, for instance, the matter can only suppress the $\nu_e \to \nu_\mu$ oscillations, while it can enhance the $\bar\nu_e \to \bar\nu_\mu$ transitions. This disparity between the behavior of neutrinos and that of antineutrinos is a consequence of the fact that the matter in the Sun or in the Earth we are interested in is not charge-symmetric (it contains e^-, p and n, but does not contain their antiparticles) and therefore the oscillations in matter are neither CP- nor CPT- invariant [44]. Thus, even in the case of 2-neutrino mixing and oscillations we have, *e.g.*, $P^{2\nu}_m(\nu_e \to \nu_{\mu(\tau)}) \neq P^{2\nu}_m(\bar\nu_e \to \bar\nu_{\mu(\tau)})$.

The matter effects in the $\nu_e \leftrightarrow \nu_{\mu(\tau)}$ ($\bar\nu_e \leftrightarrow \bar\nu_{\mu(\tau)}$) oscillations will be invariant with respect to the operation of time reversal if the N_e distribution along the neutrino path is symmetric with respect to this operation [45,56]. The latter condition is fulfilled (to a good approximation) for the N_e distribution along a path of a neutrino crossing the Earth [57].

13.3.1. *Effects of Earth matter on oscillations of neutrinos* :

The formalism we have developed can be applied, *e.g.*, to the study of matter effects in the $\nu_e \leftrightarrow \nu_{\mu(\tau)}$ ($\nu_{\mu(\tau)} \leftrightarrow \nu_e$) and $\bar\nu_e \leftrightarrow \bar\nu_{\mu(\tau)}$ ($\bar\nu_{\mu(\tau)} \leftrightarrow \bar\nu_e$) oscillations of neutrinos which traverse the Earth [58]. Indeed, the Earth density distribution in the existing Earth models [57] is assumed to be spherically symmetric and there are two major density structures - the core and the mantle, and a certain number of substructures (shells or layers). The Earth radius is $R_\oplus = 6371$ km; the Earth core has a radius of $R_c = 3486$ km, so the Earth mantle depth is 2885 km. For a spherically symmetric Earth density distribution, the neutrino trajectory in the Earth is specified by the value of the Nadir angle θ_n of the trajectory. For $\theta_n \leq 33.17^o$, or path lengths $L \geq 10660$ km, neutrinos cross the Earth core. The path length for neutrinos which cross only the Earth mantle is given by $L = 2R_\oplus \cos\theta_n$. If neutrinos cross the Earth core, the lengths of the paths in the mantle, $2L^{\mathrm{man}}$, and in the core, L^{core}, are determined by: $L^{\mathrm{man}} = R_\oplus \cos\theta_n - (R^2_c - R^2_\oplus \sin^2\theta_n)^{\frac{1}{2}}$, $L^{\mathrm{core}} = 2(R^2_c - R^2_\oplus \sin^2\theta_n)^{\frac{1}{2}}$. The mean electron number densities in the mantle and in the core according to the PREM model read [57]: $\bar N^{man}_e \cong 2.2\ \mathrm{cm}^{-3}\ \mathrm{N_A}$, $\bar N^c_e \cong 5.4\ \mathrm{cm}^{-3}\ \mathrm{N_A}$. Thus, we have $\bar N^c_e \cong 2.5\ \bar N^{man}_e$. The change of N_e from the mantle to the core can well be approximated by a step function [57]. The electron number density N_e changes relatively little around the indicated mean values along the trajectories of neutrinos which cross a substantial part of the Earth mantle, or the mantle and the core, and the two-layer constant density approximation, $N^{man}_e = const. = \tilde N^{man}_e$, $N^c_e = const. = \tilde N^c_e$, $\tilde N^{man}_e$ and $\tilde N^c_e$ being the mean densities along the given neutrino path in the Earth, was shown to be sufficiently accurate in what concerns the calculation of neutrino oscillation probabilities [45,60,63] (and references quoted in [60,63]) in a large number of specific cases. This is related to the fact that the relatively small changes of density along the path of the neutrinos in the mantle (or in the core) take place over path lengths which are typically considerably smaller than the corresponding oscillation length in matter.

In the case of 3-neutrino mixing and for neutrino energies of $E \gtrsim 2$ GeV, the effects due to Δm^2_{21} ($|\Delta m^2_{21}| \ll |\Delta m^2_{31}|$, see Eq. (13.21)) in the neutrino oscillation probabilities are sub-dominant and to leading order can be neglected: the corresponding resonance density $|N^{res}_{e21}| \lesssim 0.25\ cm^{-3}\ N_A \ll \bar N^{man,c}_e$ and the Earth matter strongly suppresses the oscillations due to Δm^2_{21}. For oscillations in vacuum this approximation is valid as long as the leading order contribution due to Δm^2_{31} in the relevant probabilities is bigger than approximately 10^{-3}. In this case the 3-neutrino $\nu_e \to \nu_{\mu(\tau)}$ ($\bar\nu_e \to \bar\nu_{\mu(\tau)}$) and $\nu_{\mu(\tau)} \to \nu_e$ ($\bar\nu_{\mu(\tau)} \to \bar\nu_e$) transition probabilities for neutrinos traversing the Earth, reduce effectively to a 2-neutrino transition probability (see, *e.g.*, [61–63]) , with Δm^2_{31} and θ_{13} playing the role of the relevant 2-neutrino vacuum oscillation parameters. The 3-neutrino oscillation probabilities of the atmospheric and accelerator $\nu_{e,\mu}$ having energy E and crossing the Earth along a trajectory characterized by a Nadir angle θ_n, for instance, have the following form:

$$P^{3\nu}_m(\nu_e \to \nu_e) \cong 1 - P^{2\nu}_m, \tag{13.40}$$

$$P^{3\nu}_m(\nu_e \to \nu_\mu) \cong P^{3\nu}_m(\nu_\mu \to \nu_e) \cong s^2_{23}\ P^{2\nu}_m\,, \qquad P^{3\nu}_m(\nu_e \to \nu_\tau) \cong c^2_{23}\ P^{2\nu}_m\,, \tag{13.41}$$

$$P^{3\nu}_m(\nu_\mu \to \nu_\mu) \cong 1 - s^4_{23}\ P^{2\nu}_m - 2c^2_{23}s^2_{23}\ \ \Big[1 - Re\ (e^{-i\kappa}A^{2\nu}_m(\nu' \to \nu'))\Big]\,, \tag{13.42}$$

$$P_m^{3\nu}(\nu_\mu \to \nu_\tau) = 1 - P_m^{3\nu}(\nu_\mu \to \nu_\mu) - P_m^{3\nu}(\nu_\mu \to \nu_e). \qquad (13.43)$$

Here $P_m^{2\nu} \equiv P_m^{2\nu}(\Delta m^2_{31}, \theta_{13}; E, \theta_n)$ is the probability of the 2-neutrino $\nu_e \to \nu' \equiv (s_{23}\nu_\mu + c_{23}\nu_\tau)$ oscillations in the Earth, and κ and $A_m^{2\nu}(\nu' \to \nu') \equiv A_m^{2\nu}$ are known phase and 2-neutrino transition probability amplitude (see, *e.g.*, [62,63]). We note that Eq. (13.40) to Eq. (13.42) are based only on the assumption that $|N_{e21}^{res}|$ is much smaller than the densities in the Earth mantle and core and does not rely on the constant density approximation. Similar results are valid for the corresponding antineutrino oscillation probabilities: one has just to replace $P_m^{2\nu}$, κ and $A_m^{2\nu}$ in the expressions given above with the corresponding quantities for antineutrinos (the latter are obtained from those for neutrinos by changing the sign in front of N_e). Obviously, we have: $P(\nu_{e(\mu)} \to \nu_{\mu(e)}), P(\bar\nu_{e(\mu)} \to \bar\nu_{\mu(e)}) \leq \sin^2\theta_{23}$, and $P(\nu_e \to \nu_\tau), P(\bar\nu_e \to \bar\nu_\tau) \leq \cos^2\theta_{23}$. The one Δm^2 dominance approximation and correspondingly Eq. (13.40) to Eq. (13.43) were used by the Super-Kamiokande Collaboration in their latest neutrino oscillation analysis of the multi-GeV atmospheric neutrino data [64].

In the case of neutrinos crossing only the Earth mantle and in the constant density approximation, $P_m^{2\nu}$ is given by the r.h.s. of Eq. (13.38) with θ and Δm^2 replaced by θ_{13} and Δm^2_{31}, while for κ and $A_m^{2\nu}$ we have (see, *e.g.*, Ref. 63):

$$\kappa \cong \frac{1}{2}[\frac{\Delta m^2_{31}}{2E}\ L + \sqrt{2}G_F\bar N_e^{man}L - \frac{\Delta M^2 L}{2E}],$$
$$A_m^{2\nu} = 1 + \left(e^{-i\frac{\Delta M^2 L}{2E}} - 1\right)\cos^2\theta'_m\ , \qquad (13.44)$$

where ΔM^2 is defined in Eq. (13.37) (with $\theta = \theta_{13}$ and $\Delta m^2 = \Delta m^2_{31}$), θ'_m is the mixing angle in the mantle which coincides in vacuum with θ_{13} (Eq. (13.35) with $N_e = \bar N_e^{man}$ and $\theta = \theta_{13}$), and $L = 2R_\oplus \cos\theta_n$ is the distance the neutrino travels in the mantle.

It follows from Eq. (13.40) and Eq. (13.41) that for $\Delta m^2_{31}\cos 2\theta_{13} > 0$, the oscillation effects of interest, *e.g.*, in the $\nu_{e(\mu)} \to \nu_{\mu(e)}$ and $\nu_e \to \nu_\tau$ transitions will be maximal if $P_m^{2\nu} \cong 1$, *i.e.*, if Eq. (13.39) leading to $\sin^2 2\theta_m \cong 1$ is fulfilled, and ii) $\cos(\Delta M^2 L/(2E)) \cong -1$. Given the value of $\bar N_e^{man}$, the first condition determines the neutrino's energy, while the second determines the path length L, for which one can have $P_m^{2\nu} \cong 1$. For $\Delta m^2_{31} \cong 2.4 \times 10^{-3}$ eV^2, $\sin^2\theta_{13} < 0.056$ (99.73% C.L.) following from the data (see Sections 13.6 and 13.7) and $\bar N_e^{man} \cong 2.2$ N$_A$cm^{-3}, one finds that $E_{res} \cong 7.2$ GeV and $L \cong 2370/\sin 2\theta_{13}$ km $\cong$ 7600 (5200) km, where we used $\sin^2\theta_{13} = 0.025$ (0.056) in the last equality. Thus, for $\Delta m^2_{31} > 0$, the Earth matter effects can amplify $P_m^{2\nu}$, and therefore $P(\nu_{e(\mu)} \to \nu_{\mu(e)})$ and $P(\nu_e \to \nu_\tau)$, significantly when the neutrinos cross only the mantle for $E \sim 7$ GeV and $L \gtrsim 5200$ km, or $\cos\theta_n \gtrsim 0.35$. If $\Delta m^2_{31} < 0$ the same considerations apply for the corresponding antineutrino oscillation probabilities $\bar P_m^{2\nu} = \bar P_m^{2\nu}(\bar\nu_e \to (s_{23}\bar\nu_\mu + c_{23}\bar\nu_\tau))$ and correspondingly for $P(\bar\nu_{e(\mu)} \to \bar\nu_{\mu(e)})$ and $P(\bar\nu_e \to \bar\nu_\tau)$. For $\Delta m^2_{31} > 0$, the $\bar\nu_{e(\mu)} \to \bar\nu_{\mu(e)}$ and $\bar\nu_e \to \bar\nu_\tau$ oscillations are suppressed by the Earth matter, while if $\Delta m^2_{31} < 0$, the same conclusion holds for the $\nu_{e(\mu)} \to \nu_{\mu(e)}$ and $\nu_e \to \nu_\tau$, oscillations.

In the case of neutrinos crossing the Earth core, new resonance-like effects become possible in the $\nu_\mu \to \nu_e$ and $\nu_e \to \nu_{\mu(\tau)}$ (or $\bar\nu_\mu \to \bar\nu_e$ and $\bar\nu_e \to \bar\nu_{\mu(\tau)}$) transitions [60,62,63,65–67]. For $\sin^2\theta_{13} < 0.05$ and $\Delta m^2_{31} > 0$, we can have [66] $P_m^{2\nu}(\Delta m^2_{31}, \theta_{13}) \cong 1$, and correspondingly maximal $P_m^{3\nu}(\nu_e \to \nu_\mu) = P_m^{3\nu}(\nu_\mu \to \nu_e) \cong s^2_{23}$, only due to the effect of maximal constructive interference between the amplitudes of the $\nu_e \to \nu'$ transitions in the Earth mantle and in the Earth core. The effect differs from the MSW one and the enhancement happens in the case of interest at a value of the energy between the MSW resonance energies corresponding to the density in the mantle and that of the core, or at a value of the resonance density N_e^{res} which lies between the values of N_e in the mantle and in the core [60]. In [60,63] the enhancement was called "neutrino oscillation length resonance", while in [62,65] the term "parametric resonance" for the same effect was used [68]. The *mantle-core enhancement effect* is caused by the existence (for a given neutrino trajectory through the Earth core) of points of resonance-like maximal neutrino conversion, $P_m^{2\nu}(\Delta m^2_{31}, \theta_{13}) = 1$, in the corresponding space of neutrino oscillation parameters [66]. For $\Delta m^2_{31} < 0$ the mantle-core enhancement can take place for the antineutrino transitions, $\bar\nu_\mu \to \bar\nu_e$ and $\bar\nu_e \to \bar\nu_{\mu(\tau)}$.

A rather complete set of values of $\Delta m^2_{31}/E > 0$ and $\sin^2 2\theta_{13}$ for which $P_m^{2\nu}(\Delta m^2_{31}, \theta_{13}) = 1$ was found in [66]. The location of these points in the $\Delta m^2_{31}/E - \sin^2 2\theta_{13}$ plane determines the regions where $P_m^{2\nu}(\Delta m^2_{31}, \theta_{13})$ is large, $P_m^{2\nu}(\Delta m^2, \theta) \gtrsim 0.5$. These regions vary slowly with the Nadir angle, being remarkably wide in the Nadir angle and rather wide in the neutrino energy [66], so that the transitions of interest can produce noticeable effects in the measured observables. For $\sin^2\theta_{13} < 0.05$, there are two sets of values of $(\Delta m^2_{31}/E, \sin^2\theta_{13})$ for which $P_m^{2\nu}(\Delta m^2_{31}, \theta_{13}) = 1$. For $\Delta m^2_{31} = 2.4 \times 10^{-3}$ eV^2 and Nadir angles, *e.g.*, θ_n=0; 13^0; 23^0, we have $P_m^{2\nu}(\Delta m^2_{31}, \theta_{13}) = 1$ at the following points in the $E - \sin^2\theta_{13}$ plane: 1) $\sin^2 2\theta_{13} =$ 0.034; 0.039; 0.051, $E \cong$ 3.3; 3.4; 3.7 GeV; and 2) $\sin^2 2\theta_{13} =$ 0.15; 0.17; 0.22, $E \cong$ 5.0; 5.3; 6.3 GeV (see Table 2 in the last article in Ref. 66; see also the last article in Ref. 67). The values of $\sin^2 2\theta_{13}$ at which the 2nd solution takes place are marginally allowed by the data.

The mantle-core enhancement of $P_m^{2\nu}$ (or $\bar P_m^{2\nu}$) is relevant, in particular, for the searches of sub-dominant $\nu_{e(\mu)} \to \nu_{\mu(e)}$ (or $\bar\nu_{e(\mu)} \to \bar\nu_{\mu(e)}$) oscillations of atmospheric neutrinos having energies $E \gtrsim 2$ GeV and crossing the Earth core on the way to the detector (see Ref. 60 to Ref. 67 and the references quoted therein). The effects of Earth matter on the oscillations of atmospheric and accelerator neutrinos have not been observed so far. At present there are no compelling evidences for oscillations of the atmospheric ν_e and/or $\bar\nu_e$.

The expression for the probability of the $\nu_e \to \nu_\mu$ oscillations taking place in the Earth mantle in the case of 3-neutrino mixing, in which both neutrino mass squared differences Δm^2_{21} and Δm^2_{31} contribute and the CP violation effects due to the Dirac phase in the neutrino mixing matrix are taken into account, has the following form in the constant density approximation and keeping terms up to second order in the two small parameters $|\alpha| \equiv |\Delta m^2_{21}|/|\Delta m^2_{31}| \ll 1$ and $\sin^2\theta_{13} \ll 1$ [69]:

$$P_m^{3\nu\ man}(\nu_e \to \nu_\mu) \cong P_0 + P_{\sin\delta} + P_{\cos\delta} + P_3\,. \qquad (13.45)$$

Here

$$P_0 = \sin^2\theta_{23}\ \frac{\sin^2 2\theta_{13}}{(A-1)^2}\ \sin^2[(A-1)\Delta]$$
$$P_3 = \alpha^2\ \cos^2\theta_{23}\ \frac{\sin^2 2\theta_{12}}{A^2}\ \sin^2(A\Delta)\,, \qquad (13.46)$$

$$P_{\sin\delta} = \alpha\ \frac{8\,J_{CP}}{A(1-A)}\,(\sin\Delta)\,(\sin A\Delta)\ (\sin[(1-A)\Delta])\ , \qquad (13.47)$$

$$P_{\cos\delta} = \alpha\ \frac{8\,J_{CP}\cot\delta}{A(1-A)}\,(\cos\Delta)\,(\sin A\Delta)\ (\sin[(1-A)\Delta])\ , \qquad (13.48)$$

where

$$\alpha = \frac{\Delta m^2_{21}}{\Delta m^2_{31}}\,,\ \Delta = \frac{\Delta m^2_{31}\,L}{4E}\,,\ A = \sqrt{2}G_{\rm F}N_e^{man}\frac{2E}{\Delta m^2_{31}}\,, \qquad (13.49)$$

and $\cot\delta = J_{CP}^{-1}{\rm Re}(U_{\mu3}U^*_{e3}U_{e2}U^*_{\mu2})$, $J_{CP} = {\rm Im}(U_{\mu3}U^*_{e3}U_{e2}U^*_{\mu2})$. The analytic expression for $P_m^{3\nu\ man}(\nu_e \to \nu_\mu)$ given above is valid for [69] neutrino path lengths in the mantle ($L \leq 10660$ km) satisfying $L \lesssim 10560$ km E[GeV] $(7.6\times10^{-5}$ eV$^2/\Delta m^2_{21})$, and energies $E \gtrsim 0.34$ GeV$(\Delta m^2_{21}/7.6 \times 10^{-5}$ eV$^2)\,(1.4$ cm$^{-3}N_A/N_e^{man})$. The expression for the $\bar\nu_e \to \bar\nu_\mu$ oscillation probability can be obtained formally from that for $P_m^{3\nu\ man}(\nu_e \to \nu_\mu)$ by making the changes $A \to -A$ and $J_{CP} \to -J_{CP}$, with $J_{CP}\cot\delta \equiv {\rm Re}(U_{\mu3}U^*_{e3}U_{e2}U^*_{\mu2})$ remaining unchanged. The term $P_{\sin\delta}$ in $P_m^{3\nu\ man}(\nu_e \to \nu_\mu)$ would be equal to zero if the Dirac phase in the neutrino mixing matrix U possesses a CP-conserving value. Even in this case, however, we have $A_{CP}^{(\mu e)\ man} \equiv (P_m^{3\nu\ man}(\nu_e \to \nu_\mu) - P_m^{3\nu\ man}(\bar\nu_e \to \bar\nu_\mu)) \neq 0$ due to the effects of the Earth matter. It will be important to experimentally disentangle the effects of the Earth matter and of J_{CP} in $A_{CP}^{(\mu e)\ man}$: this will allow to get information about the Dirac CP violation phase in U. In the vacuum limit of $N_e^{man} = 0$ ($A = 0$) we have $A_{CP}^{(\mu e)\ man} = A_{CP}^{(\mu e)}$ (see Eq. (13.18)) and only the term $P_{\sin\delta}$ contributes to the asymmetry $A_{CP}^{(\mu e)}$.

13.3.2. ***Oscillations of solar neutrinos*** :

Consider next the oscillations of solar ν_e while they propagate from the central part of the Sun, where they are produced, to the surface of the Sun [26,59] (see also, *e.g.*, [70]). Details concerning the production, spectrum, magnitude and particularities of the solar neutrino flux, the methods of detection of solar neutrinos, description of solar neutrino experiments and of the data they provided will be discussed in the next section (see also Ref. 71). The electron number density N_e changes considerably along the neutrino path in the Sun: it decreases monotonically from the value of ~ 100 cm^{-3} N_A in the center of the Sun to 0 at the surface of the Sun. According to the contemporary solar models (see, *e.g.*, [71,72]) , N_e decreases approximately exponentially in the radial direction towards the surface of the Sun:

$$N_e(t) = N_e(t_0) \exp\left\{-\frac{t-t_0}{r_0}\right\} \ , \tag{13.50}$$

where $(t - t_0) \cong d$ is the distance traveled by the neutrino in the Sun, $N_e(t_0)$ is the electron number density at the point of ν_e production in the Sun, r_0 is the scale-height of the change of $N_e(t)$ and one has [71,72] $r_0 \sim 0.1 R_\odot$.

Consider the case of 2-neutrino mixing, Eq. (13.34). Obviously, if N_e changes with t (or equivalently with the distance) along the neutrino trajectory, the matter-eigenstates, their energies, the mixing angle and the oscillation length in matter, become, through their dependence on N_e, also functions of t: $|\nu^m_{1,2}\rangle = |\nu^m_{1,2}(t)\rangle$, $E^m_{1,2} = E^m_{1,2}(t)$, $\theta_m = \theta_m(t)$ and $L_m = L_m(t)$. It is not difficult to understand qualitatively the possible behavior of the neutrino system when solar neutrinos propagate from the center to the surface of the Sun if one realizes that one is dealing effectively with a two-level system whose Hamiltonian depends on time and admits "jumps" from one level to the other (see Eq. (13.32)). Consider the case of $\Delta m^2 \cos 2\theta > 0$. Let us assume first for simplicity that the electron number density at the point of a solar ν_e production in the Sun is much bigger than the resonance density, $N_e(t_0) \gg N^{res}_e$. Actually, this is one of the cases relevant to the solar neutrinos. In this case we have $\theta_m(t_0) \cong \pi/2$ and the state of the electron neutrino in the initial moment of the evolution of the system practically coincides with the heavier of the two matter-eigenstates:

$$|\nu_e\rangle \ \cong \ |\nu^m_2(t_0)\rangle \, . \tag{13.51}$$

Thus, at t_0 the neutrino system is in a state corresponding to the "level" with energy $E^m_2(t_0)$. When neutrinos propagate to the surface of the Sun they cross a layer of matter in which $N_e = N^{res}_e$: in this layer the difference between the energies of the two "levels" $(E^m_2(t) - E^m_1(t))$ has a minimal value on the neutrino trajectory (Eq. (13.37) and Eq. (13.39)). Correspondingly, the evolution of the neutrino system can proceed basically in two ways. First, the system can stay on the "level" with energy $E^m_2(t)$, *i.e.*, can continue to be in the state $|\nu^m_2(t)\rangle$ up to the final moment t_s, when the neutrino reaches the surface of the Sun. At the surface of the Sun $N_e(t_s) = 0$ and therefore $\theta_m(t_s) = \theta$, $|\nu^m_{1,2}(t_s)\rangle \equiv |\nu_{1,2}\rangle$ and $E^m_{1,2}(t_s) = E_{1,2}$. Thus, in this case the state describing the neutrino system at t_0 will evolve continuously into the state $|\nu_2\rangle$ at the surface of the Sun. Using Eq. (13.29) with $l = e$ and $x = \mu$, it is easy to obtain the probabilities to find ν_e and ν_μ at the surface of the Sun:

$$\begin{aligned} P(\nu_e \to \nu_e; t_s, t_0) &\cong |\langle \nu_e | \nu_2 \rangle|^2 = \sin^2\theta \\ P(\nu_e \to \nu_\mu; t_s, t_0) &\cong |\langle \nu_\mu | \nu_2 \rangle|^2 = \cos^2\theta \, . \end{aligned} \tag{13.52}$$

It is clear that under the assumption made and if $\sin^2\theta \ll 1$, practically a total $\nu_e \to \nu_\mu$ conversion is possible. This type of evolution of the neutrino system and the $\nu_e \to \nu_\mu$ transitions taking place during the evolution, are called [26] "adiabatic." They are characterized by the fact that the probability of the "jump" from the upper "level" (having energy $E^m_2(t)$) to the lower "level" (with energy $E^m_1(t)$), P', or equivalently the probability of the $\nu^m_2(t_0) \to \nu^m_1(t_s)$ transition, $P' \equiv P'(\nu^m_2(t_0) \to \nu^m_1(t_s))$, on the whole neutrino trajectory is negligible:

$$P' \equiv P'(\nu^m_2(t_0) \to \nu^m_1(t_s)) \cong 0 \ : \ \textit{adiabatic transitions} \, . \tag{13.53}$$

The second possibility is realized if in the resonance region, where the two "levels" approach each other closest the system "jumps" from the upper "level" to the lower "level" and after that continues to be in the state $|\nu^m_1(t)\rangle$ until the neutrino reaches the surface of the Sun. Evidently, now we have $P' \equiv P'(\nu^m_2(t_0) \to \nu^m_1(t_s)) \sim 1$. In this case the neutrino system ends up in the state $|\nu^m_1(t_s)\rangle \equiv |\nu_1\rangle$ at the surface of the Sun and

$$\begin{aligned} P(\nu_e \to \nu_e; t_s, t_0) &\cong |\langle \nu_e | \nu_1 \rangle|^2 = \cos^2\theta \\ P(\nu_e \to \nu_\mu; t_s, t_0) &\cong |\langle \nu_\mu | \nu_1 \rangle|^2 = \sin^2\theta \, . \end{aligned} \tag{13.54}$$

Obviously, if $\sin^2\theta \ll 1$, practically no transitions of the solar ν_e into ν_μ will occur. The considered regime of evolution of the neutrino system and the corresponding $\nu_e \to \nu_\mu$ transitions are usually referred to as "extremely nonadiabatic."

Clearly, the value of the "jump" probability P' plays a crucial role in the the $\nu_e \to \nu_\mu$ transitions: it fixes the type of the transition and determines to a large extent the $\nu_e \to \nu_\mu$ transition probability [59,73,74]. We have considered above two limiting cases. Obviously, there exists a whole spectrum of possibilities since P' can have any value from 0 to $\cos^2\theta$ [75,76]. In general, the transitions are called "nonadiabatic" if P' is non-negligible.

Numerical studies have shown [26] that solar neutrinos can undergo both adiabatic and nonadiabatic $\nu_e \to \nu_\mu$ transitions in the Sun and the matter effects can be substantial in the solar neutrino oscillations for 10^{-8} eV$^2 \lesssim \Delta m^2 \lesssim 10^{-4}$ eV^2, $10^{-4} \lesssim \sin^2 2\theta < 1.0$.

The condition of adiabaticity of the solar ν_e transitions in Sun can be written as [59,73]

$$\gamma(t) \equiv \sqrt{2} G_F \frac{(N^{res}_e)^2}{|\dot{N}_e(t)|} \tan^2 2\theta \left(1 + \tan^{-2} 2\theta_m(t)\right)^{\frac{3}{2}} \ \gg 1$$
$$\text{adiabatic transitions} \, , \tag{13.55}$$

while if $\gamma(t) \lesssim 1$ the transitions are nonadiabatic (see also Ref. 76), where $\dot{N}_e(t) \equiv \frac{d}{dt} N_e(t)$. Condition in Eq. (13.55) implies that the $\nu_e \to \nu_{\mu(\tau)}$ transitions in the Sun will be adiabatic if $N_e(t)$ changes sufficiently slowly along the neutrino path. In order for the transitions to be adiabatic, condition in Eq. (13.55) has to be fulfilled at any point of the neutrino's path in the Sun.

Actually, the system of evolution equations Eq. (13.32) can be solved exactly for N_e changing exponentially, Eq. (13.50), along the neutrino path in the Sun [75,77]. More specifically, the system in Eq. (13.32) is equivalent to one second order differential equation (with appropriate initial conditions). The latter can be shown [78] to coincide in form, in the case of N_e given by Eq. (13.50), with the Schroedinger equation for the radial part of the nonrelativistic wave function of the Hydrogen atom [79]. On the basis of the exact solution, which is expressed in terms of confluent hypergeometric functions, it was possible to derive a complete, simple and very accurate analytic description of the matter-enhanced transitions of solar neutrinos in the Sun for any values of Δm^2 and θ [75,76,80,81] (see also [26,59,74,82,83]) .

The probability that a ν_e, produced at time t_0 in the central part of the Sun, will not transform into $\nu_{\mu(\tau)}$ on its way to the surface of the Sun (reached at time t_s) is given by

$$P^{2\nu}_\odot(\nu_e \to \nu_e; t_s, t_0) = \bar{P}^{2\nu}_\odot(\nu_e \to \nu_e; t_s, t_0) + \ \textit{Oscillating terms.} \tag{13.56}$$

Here

$$\bar{P}^{2\nu}_\odot(\nu_e \to \nu_e; t_s, t_0) \equiv \bar{P}_\odot = \frac{1}{2} + \left(\frac{1}{2} - \mathrm{P}'\right) \cos 2\theta_m(t_0) \cos 2\theta \ , \tag{13.57}$$

is the average survival probability for ν_e having energy $\mathrm{E} \cong \mathrm{p}$ [74], where

$$P' = \frac{\exp\left[-2\pi \mathrm{r}_0 \frac{\Delta m^2}{2E} \sin^2\theta\right] - \exp\left[-2\pi \mathrm{r}_0 \frac{\Delta m^2}{2E}\right]}{1 - \exp\left[-2\pi \mathrm{r}_0 \frac{\Delta m^2}{2E}\right]} \, , \tag{13.58}$$

is [75] the "jump" probability for exponentially varying N_e, and $\theta_m(t_0)$ is the mixing angle in matter at the point of ν_e production [82]. The expression for $\bar{P}^{2\nu}_{\odot}(\nu_e \to \nu_e; t_s, t_0)$ with P' given by Eq. (13.58) is valid for $\Delta m^2 > 0$, but for both signs of $\cos 2\theta \neq 0$ [75,83]; it is valid for any given value of the distance along the neutrino trajectory and does not take into account the finite dimensions of the region of ν_e production in the Sun. This can be done by integrating over the different neutrino paths, *i.e.*, over the region of ν_e production.

The oscillating terms in the probability $P^{2\nu}_{\odot}(\nu_e \to \nu_e; t_s, t_0)$ [80,78] were shown [81] to be strongly suppressed for $\Delta m^2 \gtrsim 10^{-7}$ eV^2 by the various averagings one has to perform when analyzing the solar neutrino data. The current solar neutrino and KamLAND data suggest that $\Delta m^2 \cong 7.6 \times 10^{-5}$ eV^2. For $\Delta m^2 \gtrsim 10^{-7}$ eV^2, the averaging over the region of neutrino production in the Sun *etc.* renders negligible all interference terms which appear in the probability of ν_e survival due to the $\nu_e \leftrightarrow \nu_{\mu(\tau)}$ oscillations in vacuum taking place on the way of the neutrinos from the surface of the Sun to the surface of the Earth. Thus, the probability that ν_e will remain ν_e while it travels from the central part of the Sun to the surface of the Earth is effectively equal to the probability of survival of the ν_e while it propagates from the central part to the surface of the Sun and is given by the average probability $\bar{P}_{\odot}(\nu_e \to \nu_e; t_s, t_0)$ (determined by Eq. (13.57) and Eq. (13.58)).

If the solar ν_e transitions are adiabatic ($P' \cong 0$) and $\cos 2\theta_m(t_0) \cong -1$ (*i.e.*, $N_e(t_0)/|N_e^{res}| \gg 1, |\tan 2\theta|$, the ν_e are born "above" (in N_e) the resonance region), one has [26]

$$\bar{P}^{2\nu}(\nu_e \to \nu_e; t_s, t_0) \cong \frac{1}{2} - \frac{1}{2}\cos 2\theta. \tag{13.59}$$

The regime under discussion is realised for $\sin^2 2\theta \cong 0.8$ (suggested by the data, Section 13.4), if $E/\Delta m^2$ lies approximately in the range $(2 \times 10^4 - 3 \times 10^7)$ MeV/eV^2 (see Ref. 76). This result is relevant for the interpretation of the Super-Kamiokande and SNO solar neutrino data. We see that depending on the sign of $\cos 2\theta \neq 0$, $\bar{P}^{2\nu}(\nu_e \to \nu_e)$ is either bigger or smaller than 1/2. It follows from the solar neutrino data that in the range of validity (in $E/\Delta m^2$) of Eq. (13.59) we have $\bar{P}^{2\nu}(\nu_e \to \nu_e) \cong 0.3$. Thus, the possibility of $\cos 2\theta \leq 0$ is ruled out by the data. Given the choice $\Delta m^2 > 0$ we made, the data imply that $\Delta m^2 \cos 2\theta > 0$.

If $E/\Delta m^2$ is sufficiently small so that $N_e(t_0)/|N_e^{res}| \ll 1$, we have $P' \cong 0$, $\theta_m(t_0) \cong \theta$ and the oscillations take place in the Sun as in vacuum [26]:

$$\bar{P}^{2\nu}(\nu_e \to \nu_e; t_s, t_0) \cong 1 - \frac{1}{2}\sin^2 2\theta\,, \tag{13.60}$$

which is the average two-neutrino vacuum oscillation probability. This expression describes with good precision the transitions of the solar *pp* neutrinos (Section 13.4). The extremely nonadiabatic ν_e transitions in the Sun, characterised by $\gamma(t) \ll 1$, are also described by the average vacuum oscillation probability (Eq. (13.60)) (for $\Delta m^2 \cos 2\theta > 0$ in this case we have (see *e.g.*, [75,76]) $\cos 2\theta_m(t_0) \cong -1$ and $P' \cong \cos^2\theta$).

The probability of ν_e survival in the case 3-neutrino mixing takes a simple form for $|\Delta m^2_{31}| \cong 2.4 \times 10^{-3}$ eV$^2 \gg |\Delta m^2_{21}|$. Indeed, for the energies of solar neutrinos $E \lesssim 10$ MeV, N^{res} corresponding to $|\Delta m^2_{31}|$ satisfies $N^{res}_{e31} \gtrsim 10^3$ cm^{-3} N$_A$ and is by a factor of 10 bigger than N_e in the center of the Sun. As a consequence, the oscillations due to Δm^2_{31} proceed as in vacuum. The oscillation length associated with $|\Delta m^2_{31}|$ satisfies $L^v_{31} \lesssim 10$ km $\ll \Delta R$, ΔR being the dimension of the region of ν_e production in the Sun. We have for the different components of the solar ν_e flux [71] $\Delta R \cong (0.04 - 0.20) R_{\odot}$. Therefore the averaging over ΔR strongly suppresses the oscillations due to Δm^2_{31} and we get [61,84]:

$$P^{3\nu}_{\odot} \cong \sin^4\theta_{13} + \cos^4\theta_{13}\ P^{2\nu}_{\odot}(\Delta m^2_{21}, \theta_{12}; N_e \cos^2\theta_{13})\,, \tag{13.61}$$

where $P^{2\nu}_{\odot}(\Delta m^2_{21}, \theta_{12}; N_e \cos^2\theta_{13})$ is given by Eq. (13.56) to Eq. (13.58) in which $\Delta m^2 = \Delta m^2_{21}$, $\theta = \theta_{12}$ and the solar e^- number density N_e is replaced by $N_e \cos^2\theta_{13}$. Thus, the solar ν_e transitions observed by the Super-Kamiokande and SNO experiments are described approximately by:

$$P^{3\nu}_{\odot} \cong \sin^4\theta_{13} + \cos^4\theta_{13}\ \sin^2\theta_{12}\,. \tag{13.62}$$

The data show that $P^{3\nu}_{\odot} \cong 0.3$, which is a strong evidence for matter effects in the solar ν_e transitions [85] since in the case of oscillations in vacuum $P^{3\nu}_{\odot} \cong \sin^4\theta_{13} + (1 - 0.5\sin^2 2\theta_{12})\cos^4\theta_{13} \gtrsim 0.48$, where we used $\sin^2\theta_{13} < 0.056$ and $\sin^2 2\theta_{12} \lesssim 0.93$.

13.4. Measurements of $\Delta m^2_{\odot}$ and $\theta_{\odot}$

13.4.1. *Solar neutrino observations* :

Observation of solar neutrinos directly addresses the theory of stellar structure and evolution, which is the basis of the standard solar model (SSM). The Sun as a well-defined neutrino source also provides extremely important opportunities to investigate nontrivial neutrino properties such as nonzero mass and mixing, because of the wide range of matter density and the great distance from the Sun to the Earth.

The solar neutrinos are produced by some of the fusion reactions in the pp chain or CNO cycle. The combined effect of these reactions is written as

$$4p \to {}^4\mathrm{He} + 2e^+ + 2\nu_e. \tag{13.63}$$

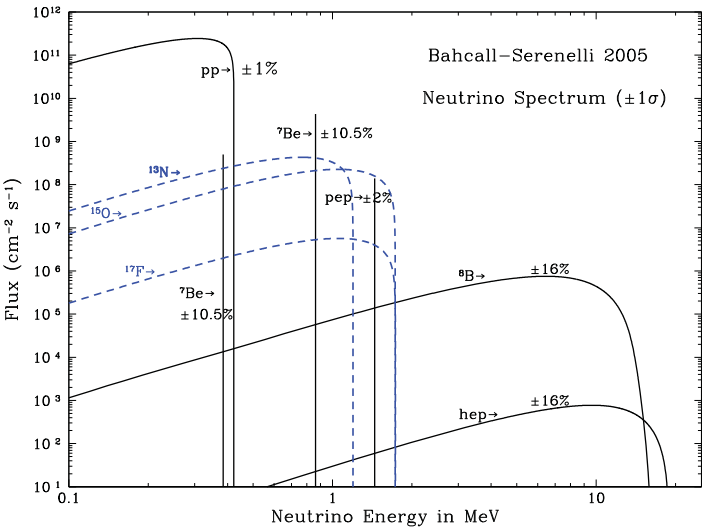

Figure 13.2: The solar neutrino spectrum predicted by the BS05(OP) standard solar model [86]. The neutrino fluxes are given in units of cm^{-2}s^{-1}MeV^{-1} for continuous spectra and cm^{-2}s^{-1} for line spectra. The numbers associated with the neutrino sources show theoretical errors of the fluxes. This figure is taken from the late John Bahcall's web site, `http://www.sns.ias.edu/~jnb/`.

Positrons annihilate with electrons. Therefore, when considering the solar thermal energy generation, a relevant expression is

$$4p + 2e^- \to {}^4\mathrm{He} + 2\nu_e + 26.73\ \mathrm{MeV} - E_{\nu}\,, \tag{13.64}$$

where E_{ν} represents the energy taken away by neutrinos, with an average value being $\langle E_{\nu} \rangle \sim 0.6$ MeV. There have been efforts to calculate solar neutrino fluxes from these reactions on the basis of SSM. A variety of input information is needed in the evolutionary calculations. The most elaborate SSM calculations have been developed by Bahcall and his collaborators, who define their SSM as the solar model which is constructed with the best available physics and input data. Therefore, their SSM calculations have been rather frequently updated. SSM's labelled as BS05(OP) [86], BSB06(GS) and BSB06(AGS) [72], and BPS08(GS) and BPS08(AGS) [87] represent recent model calculations. (Bahcall passed away in 2005, but his program to improve SSM is still pursued by his collaborators.)

Here, "OP" means that newly calculated radiative opacities from the "Opacity Project" are used. The later models are also calculated with OP opacities. "GS" and "AGS" refer to old and new determinations of solar abundances of heavy elements. There are significant differences between the old, higher heavy element abundances (GS) and the new, lower heavy element abundances (AGS). The BS05(OP) model was calculated with GS, but it adopted conservative theoretical uncertainties in the solar neutrino fluxes to account for the differences between GS and AGS. The models with GS are consistent with helioseismological data, but the models with AGS are not. The BPS08(GS) model may be considered to be the currently preferred SSM. Its prediction for the fluxes from neutrino-producing reactions is given in Table 13.2. Fig. 13.2 shows the solar-neutrino spectra calculated with the BS05(OP) model which is similar to the BPS08(GS) model.

Table 13.2: Neutrino-producing reactions in the Sun (first column) and their abbreviations (second column). The neutrino fluxes predicted by the BPS08(GS) model [87] are listed in the third column.

Reaction	Abbr.	Flux ($\mathrm{cm^{-2}\ s^{-1}}$)
$pp \to d\, e^+\, \nu$	*pp*	$5.97(1 \pm 0.006) \times 10^{10}$
$pe^- p \to d\, \nu$	*pep*	$1.41(1 \pm 0.011) \times 10^{8}$
$^3\mathrm{He}\ p \to {}^4\mathrm{He}\ e^+\nu$	*hep*	$7.90(1 \pm 0.15) \times 10^{3}$
$^7\mathrm{Be}\ e^- \to {}^7\mathrm{Li}\ \nu + (\gamma)$	^{7}Be	$5.07(1 \pm 0.06) \times 10^{9}$
$^8\mathrm{B} \to {}^8\mathrm{Be}^*\ e^+\nu$	^{8}B	$5.94(1 \pm 0.11) \times 10^{6}$
$^{13}\mathrm{N} \to {}^{13}\mathrm{C}\ e^+\nu$	^{13}N	$2.88(1 \pm 0.15) \times 10^{8}$
$^{15}\mathrm{O} \to {}^{15}\mathrm{N}\ e^+\nu$	^{15}O	$2.15(1^{+0.17}_{-0.16}) \times 10^{8}$
$^{17}\mathrm{F} \to {}^{17}\mathrm{O}\ e^+\nu$	^{17}F	$5.82(1^{+0.19}_{-0.17}) \times 10^{6}$

So far, solar neutrinos have been observed by chlorine (Homestake) and gallium (SAGE, GALLEX, and GNO) radiochemical detectors and water Cherenkov detectors using light water (Kamiokande and Super-Kamiokande) and heavy water (SNO). Recently, a liquid scintillation detector (Borexino) successfully observed low energy solar neutrinos.

A pioneering solar neutrino experiment by Davis and collaborators at Homestake using the ^{37}Cl - ^{37}Ar method proposed by Pontecorvo [88] started in the late 1960's. This experiment exploited ν_e absorption on ^{37}Cl nuclei followed by the produced ^{37}Ar decay through orbital e^- capture,

$$\nu_e + {}^{37}\mathrm{Cl} \to {}^{37}\mathrm{Ar} + e^- \ \text{(threshold 814 keV)}. \tag{13.65}$$

The ^{37}Ar atoms produced are radioactive, with a half life ($\tau_{1/2}$) of 34.8 days. After an exposure of the detector for two to three times $\tau_{1/2}$, the reaction products were chemically extracted and introduced into a low-background proportional counter, where they were counted for a sufficiently long period to determine the exponentially decaying signal and a constant background. Solar-model calculations predict that the dominant contribution in the chlorine experiment came from ^{8}B neutrinos, but ^{7}Be, *pep*, ^{13}N, and ^{15}O neutrinos also contributed (for notations, refer to Table 13.2).

From the very beginning of the solar-neutrino observation [89], it was recognized that the observed flux was significantly smaller than the SSM prediction, provided nothing happens to the electron neutrinos after they are created in the solar interior. This deficit has been called "the solar-neutrino problem."

Gallium experiments (GALLEX and GNO at Gran Sasso in Italy and SAGE at Baksan in Russia) utilize the reaction

$$\nu_e + {}^{71}\mathrm{Ga} \to {}^{71}\mathrm{Ge} + e^- \ \text{(threshold 233 keV)}. \tag{13.66}$$

They are sensitive to the most abundant *pp* solar neutrinos. However, the solar-model calculations predict almost half of the capture rate in gallium is due to other solar neutrinos. GALLEX presented the first evidence of *pp* solar-neutrino observation in 1992 [7]. The GALLEX Collaboration finished observations in early 1997 [8]. Since April, 1998, a newly defined collaboration, GNO (Gallium Neutrino Observatory) continued the observations until April 2003. The GNO results are published in Ref. 9. The GNO + GALLEX joint analysis results are also presented in Ref. 9. SAGE initially reported very low flux [90], but later observed similar flux to that of GALLEX. The latest SAGE results are published in Ref. 6. The SAGE experiment continues to collect data.

In 1987, the Kamiokande experiment in Japan succeeded in real-time solar neutrino observation, utilizing νe scattering,

$$\nu_x + e^- \to \nu_x + e^-\,, \tag{13.67}$$

in a large water-Cherenkov detector. This experiment takes advantage of the directional correlation between the incoming neutrino and the recoil electron. This feature greatly helps the clear separation of the solar-neutrino signal from the background. The Kamiokande result gave the first direct evidence that neutrinos come from the direction of the Sun [91]. Later, the high-statistics Super-Kamiokande experiment [92,93] with a 50-kton water Cherenkov detector replaced the Kamiokande experiment. Due to the high thresholds (7 MeV in Kamiokande and 5 MeV at present in Super-Kamiokande) the experiments observe pure ^{8}B solar neutrinos. It should be noted that the reaction (Eq. (13.67)) is sensitive to all active neutrinos, $x = e$, μ, and τ. However, the sensitivity to ν_μ and ν_τ is much smaller than the sensitivity to ν_e, $\sigma(\nu_{\mu,\tau}e) \approx 0.16\,\sigma(\nu_e e)$.

In 1999, a new real time solar-neutrino experiment, SNO (Sudbury Neutrino Observatory), in Canada started observation. This experiment used 1000 tons of ultra-pure heavy water (D_2O) contained in a spherical acrylic vessel, surrounded by an ultra-pure H_2O shield. SNO measured ^{8}B solar neutrinos via the charged-current (CC) and neutral-current (NC) reactions

$$\nu_e + d \to e^- + p + p \qquad \text{(CC)}\,, \tag{13.68}$$

and

$$\nu_x + d \to \nu_x + p + n \qquad \text{(NC)}\,, \tag{13.69}$$

as well as νe scattering, (Eq. (13.67)). The CC reaction, (Eq. (13.68)), is sensitive only to ν_e, while the NC reaction, (Eq. (13.69)), is sensitive to all active neutrinos. This is a key feature to solve the solar neutrino problem. If it is caused by flavour transitions such as neutrino oscillations, the solar neutrino fluxes measured by CC and NC reactions would show a significant difference.

The Q-value of the CC reaction is -1.4 MeV and the e^- energy is strongly correlated with the ν_e energy. Thus, the CC reaction provides an accurate measure of the shape of the ^{8}B neutrino spectrum. The contributions from the CC reaction and νe scattering can be distinguished by using different $\cos\,\theta$ distributions, where θ is the angle of the e^- momentum with respect to the Sun-Earth axis. While the νe scattering events have a strong forward peak, CC events have an approximate angular distribution of $1 - 1/3\,\cos\theta$.

The neutrino energy threshold of the NC reaction is 2.2 MeV. In the pure D_2O [11,12], the signal of the NC reaction was neutron capture in deuterium, producing a 6.25-MeV γ-ray. In this case, the capture efficiency was low and the deposited energy was close to the detection threshold of 5 MeV. In order to enhance both the capture efficiency and the total γ-ray energy (8.6 MeV), 2 tons of NaCl were added to the heavy water in the second phase of the experiment [94]. Subsequently NaCl was removed and an array of ^{3}He neutron counters were installed for the third phase measurement [95]. These neutron counters provided independent NC measurement with different systematics from that of the second phase, and thus strengthened the reliability of the NC measurement.

Another real time solar neutrino experiment, Borexino at Gran Sasso in Italy, started solar neutrino observation in 2007. This experiment measures solar neutrinos via νe scattering in 300 tons of ultra-pure liquid scintillator. With a detection threshold as low as 250 keV, the flux of monochromatic 0.862 MeV ^{7}Be solar neutrinos has been directly observed for the first time. The observed

energy spectrum shows the characteristic Compton-edge over the background [96]. Measurements of low energy solar neutrinos are important not only to test the SSM further, but also to study the MSW effect over the energy region spanning from sub-MeV to 10 MeV.

Table 13.3: Results from radiochemical solar-neutrino experiments. The predictions of a recent standard solar model BPS08(GS) are also shown. The first and the second errors in the experimental results are the statistical and systematic errors, respectively. SNU (Solar Neutrino Unit) is defined as 10^{-36} neutrino captures per atom per second.

	^{37}Cl→^{37}Ar (SNU)	^{71}Ga→^{71}Ge (SNU)
Homestake [4]	$2.56 \pm 0.16 \pm 0.16$	–
GALLEX [8]	–	$77.5 \pm 6.2^{+4.3}_{-4.7}$
GNO [9]	–	$62.9^{+5.5}_{-5.3} \pm 2.5$
GNO+GALLEX [9]	–	$69.3 \pm 4.1 \pm 3.6$
SAGE [6]	–	$65.4^{+3.1+2.6}_{-3.0-2.8}$
SSM [BPS08(GS)] [87]	$8.46^{+0.87}_{-0.88}$	$127.9^{+8.1}_{-8.2}$

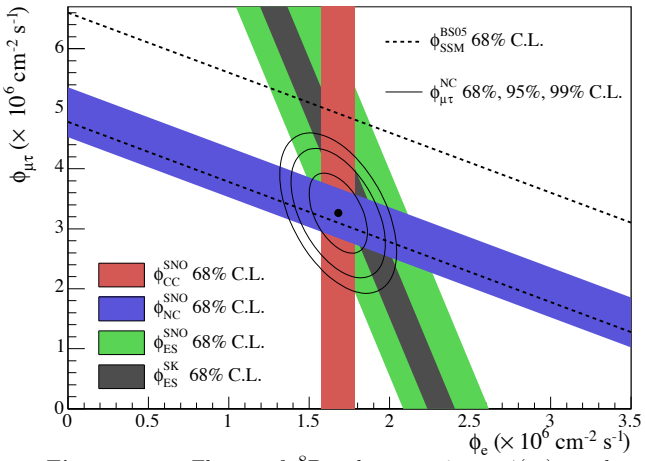

Figure 13.3: Fluxes of ^{8}B solar neutrinos, $\phi(\nu_e)$, and $\phi(\nu_{\mu \text{ or } \tau})$, deduced from the SNO's CC, ES, and NC results of the salt phase measurement [94]. The Super-Kamiokande ES flux is from Ref. 99. The BS05(OP) standard solar model prediction [86] is also shown. The bands represent the 1σ error. The contours show the 68%, 95%, and 99% joint probability for $\phi(\nu_e)$ and $\phi(\nu_{\mu \text{ or } \tau})$. The figure is from Ref. 94.

Table 13.3 and Table 13.4 show the results from solar-neutrino experiments compared with the SSM calculations. Table 13.4 includes the results from the SNO group's recent joint analysis of the SNO Phase I and Phase II data with the analysis threshold as low as 3.5 MeV (effective electron kinetic energy) and significantly improved systematic uncertainties [97]. It is seen from these tables that the results from all the solar-neutrino experiments, except SNO's NC result, indicate significantly less flux than expected from the solar-model predictions.

Table 13.4: Results from real time solar-neutrino experiments. The predictions of a recent standard solar model BPS08(GS) are also shown. The first and the second errors in the experimental results are the statistical and systematic errors, respectively.

	Reaction	^{8}B ν flux (10^6cm^{-2}s^{-1})	^{7}Be ν flux (10^9cm^{-2}s^{-1})
Kamiokande [5]	ν_e	$2.80 \pm 0.19 \pm 0.33$	–
Super-Kamiokande [93]	ν_e	$2.35 \pm 0.02 \pm 0.08$	–
SNO Phase I [12]	*CC*	$1.76^{+0.06}_{-0.05} \pm 0.09$	–
(pure D_20)	ν_e	$2.39^{+0.24}_{-0.23} \pm 0.12$	–
	NC	$5.09^{+0.44+0.46}_{-0.43-0.43}$	–
SNO Phase II [94]	*CC*	$1.68 \pm 0.06^{+0.08}_{-0.09}$	–
(NaCl in D_2O)	ν_e	$2.35 \pm 0.22 \pm 0.15$	–
	NC	$4.94 \pm 0.21^{+0.38}_{-0.34}$	–
SNO Phase III [95]	*CC*	$1.67^{+0.05+0.07}_{-0.04-0.08}$	–
(^{3}He counters)	ν_e	$1.77^{+0.24+0.09}_{-0.21-0.10}$	–
	NC	$5.54^{+0.33+0.36}_{-0.31-0.34}$	–
SNO Phase I+II [97]	*NC*	$5.140^{+0.160+0.132}_{-0.158-0.117}$	–
(Joint Analysis)	$\phi_{^8B}$ from fit to all data	$5.046^{+0.159+0.107}_{-0.152-0.123}$	–
Borexino [96]	ν_e	–	3.36 ± 0.34
SSM [BPS08(GS)] [87]	–	$5.94(1 \pm 0.11)$	$5.07(1 \pm 0.06)$

13.4.2. ***Evidence for solar neutrino flavour conversion*** :

Solar neutrino experiments achieved remarkable progress in the past ten years, and the solar-neutrino problem, which had remained unsolved for more than 30 years, has been understood as due to neutrino flavour conversion. In 2001, the initial SNO CC result combined with the Super-Kamiokande's high-statistics νe elastic scattering result [98] provided direct evidence for flavour conversion of solar neutrinos [11]. Later, SNO's NC measurements further strengthened this conclusion [12,94,95]. From the salt-phase measurement [94], the fluxes measured with CC, ES, and NC events were obtained as

$$\phi_{\rm SNO}^{\rm CC} = (1.68 \pm 0.06^{+0.08}_{-0.09}) \times 10^6 {\rm cm}^{-2}{\rm s}^{-1} \ , \tag{13.70}$$

$$\phi_{\rm SNO}^{\rm ES} = (2.35 \pm 0.22 \pm 0.15) \times 10^6 {\rm cm}^{-2}{\rm s}^{-1} \ , \tag{13.71}$$

$$\phi_{\rm SNO}^{\rm NC} = (4.94 \pm 0.21^{+0.38}_{-0.34}) \times 10^6 {\rm cm}^{-2}{\rm s}^{-1} \ , \tag{13.72}$$

where the first errors are statistical and the second errors are systematic. In the case of $\nu_e \to \nu_{\mu,\tau}$ transitions, Eq. (13.72) is a mixing-independent result and therefore tests solar models. It shows good agreement with the ^{8}B solar-neutrino flux predicted by the solar model [86]. Fig. 13.3 shows the salt phase result of $\phi(\nu_{\mu \text{ or } \tau})$ versus the flux of electron neutrinos $\phi(\nu_e)$ with the 68%, 95%, and 99% joint probability contours. The flux of non-ν_e active neutrinos, $\phi(\nu_{\mu \text{ or } \tau})$, can be deduced from these results. It is

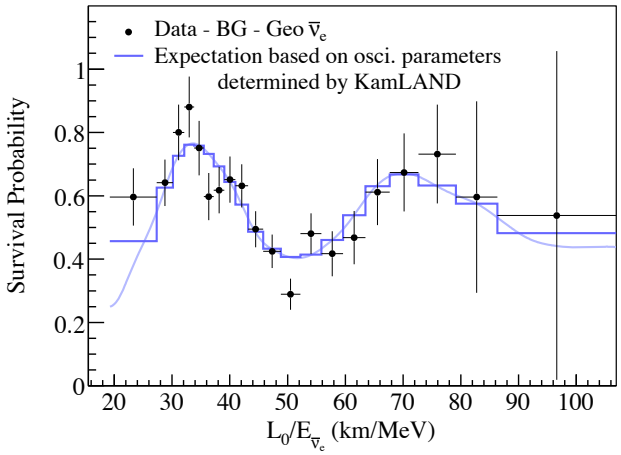

Figure 13.4: The ratio of the background and geoneutrino-subtracted $\bar{\nu}_e$ spectrum to the predicted one without oscillations (survival probability) as a function of L_0/E, where L_0=180 km. The curves show the best-fit expectations for $\bar{\nu}_e$ oscillations. The figure is from Ref. [101].

$$\phi(\nu_{\mu \text{ or } \tau}) = \left(3.26 \pm 0.25^{+0.40}_{-0.35}\right) \times 10^6 {\rm cm}^{-2}{\rm s}^{-1}. \tag{13.73}$$

The non-zero $\phi(\nu_{\mu \text{ or } \tau})$ is strong evidence for neutrino flavor conversion. These results are consistent with those expected from the LMA (large mixing angle) solution of solar neutrino oscillation in matter [25,26] with $\Delta m^2_\odot \sim 5 \times 10^{-5}$ eV^2 and $\tan^2\theta_\odot \sim 0.45$. However, with the SNO data alone, the possibility of other solutions cannot be excluded with sufficient statistical significance.

13.4.3. ***KamLAND experiment*** : KamLAND is a 1-kton ultra-pure liquid scintillator detector located at the old Kamiokande's site in Japan. The primary goal of the KamLAND experiment was a long-baseline (flux-weighted average distance of $\sim$ 180 km) neutrino oscillation studies using $\bar{\nu}_e$'s emitted from nuclear power reactors. The reaction $\bar{\nu}_e + p \to e^+ + n$ is used to detect reactor $\bar{\nu}_e$'s and a delayed coincidence of the positron with a 2.2 MeV γ-ray from neutron capture on a proton is used to reduce the backgrounds. With the reactor $\bar{\nu}_e$'s energy spectrum ($<$ 8 MeV) and a prompt-energy analysis threshold of 2.6 MeV, this experiment has a sensitive Δm^2 range down to $\sim 10^{-5}$ eV^2. Therefore, if the LMA solution is the real solution of the solar neutrino problem, KamLAND should observe reactor $\bar{\nu}_e$ disappearance, assuming CPT invariance.

The first KamLAND results [15] with 162 ton·yr exposure were reported in December 2002. The ratio of observed to expected (assuming no $\bar{\nu}_e$ oscillations) number of events was

$$\frac{N_{\rm obs} - N_{\rm BG}}{N_{\rm NoOsc}} = 0.611 \pm 0.085 \pm 0.041 \tag{13.74}$$

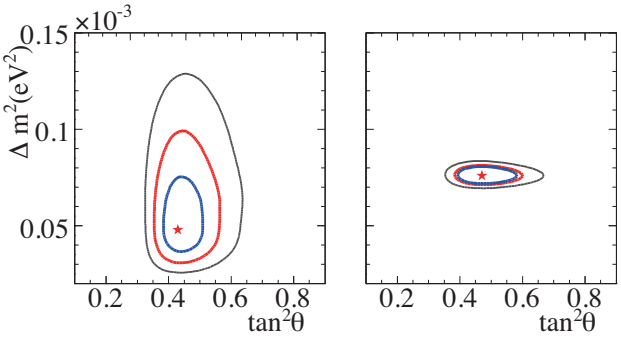

Figure 13.5: 68%, 95%, and 99.73% confidence level allowed parameter regions as well as the best-fit points are shown for (left) global solar neutrino data analysis and (right) global solar neutrino + KamLAND data analysis. This figure is taken from Ref. 95.

with obvious notation. This result showed clear evidence of an event deficit expected from neutrino oscillations. The 95% CL allowed regions are obtained from the oscillation analysis with the observed event rates and positron spectrum shape. A combined global solar + KamLAND analysis showed that the LMA is a unique solution to the solar neutrino problem with $> 5\sigma$ CL [100]. With increased statistics [16,101], KamLAND observed not only the distortion of the $\bar{\nu}_e$ spectrum, but also the periodic feature of the $\bar{\nu}_e$ survival probability expected from neutrino oscillations for the first time (see Fig. 13.4). A two-neutrino oscillation analysis gave $\Delta m^2_\odot = 7.58^{+0.14+0.15}_{-0.13-0.15} \times 10^{-5}$ eV^2 and $\tan^2\theta_\odot = 0.56^{+0.10+0.10}_{-0.07-0.06}$.

13.4.4. ***Global neutrino oscillation analysis*** :

The SNO Collaboration updated [95] a two-neutrino oscillation analysis including all the solar neutrino data (SNO, Super-Kamiokande, chlorine, gallium, and Borexino) and the KamLAND data [101]. The best fit parameters obtained from this global solar + KamLAND analysis are $\Delta m^2_\odot = 7.59^{+0.19}_{-0.21} \times 10^{-5}$ eV^2 and $\theta_\odot = 34.4^{+1.3}_{-1.2}$ degrees ($\tan^2\theta_\odot = 0.468^{+0.048}_{-0.040}$). The global solar analysis, however, gives the best fit parameters of $\Delta m^2_\odot = 4.90 \times 10^{-5}$ eV^2 and $\tan^2\theta_\odot = 0.437$. The allowed parameter regions obtained from these two analyses are shown in Fig. 13.5. The best-fit values of $\Delta m^2_\odot$ from the two analyses show a rather large difference. However, according to the recent SNO's two-neutrino oscillation analyses using its Phase I and Phase II joint analysis [97] results, this difference has become smaller. Namely, the best fit parameters obtained from the new global solar + KamLAND analysis are $\Delta m^2_\odot = 7.59^{+0.20}_{-0.21} \times 10^{-5}$ eV^2 and $\theta_\odot = 34.06^{+1.16}_{-0.84}$ degrees ($\tan^2\theta_\odot = 0.457^{+0.040}_{-0.029}$), and those from the global solar analysis are $\Delta m^2_\odot = 5.89^{+2.13}_{-2.16} \times 10^{-5}$ eV^2 and $\tan^2\theta_\odot = 0.457^{+0.038}_{-0.041}$ [97].

13.5. Measurements of $|\Delta m^2_{\rm A}|$ and $\theta_{\rm A}$

13.5.1. ***Atmospheric neutrino results*** :

The first compelling evidence for the neutrino oscillation was presented by the Super-Kamiokande Collaboration in 1998 [13] from the observation of atmospheric neutrinos produced by cosmic-ray interactions in the atmosphere. The zenith-angle distributions of the μ-like events which are mostly muon-neutrino and muon antineutrino initiated charged-current interactions, showed a clear deficit compared to the no-oscillation expectation. Note that a water Cherenkov detector cannot measure the charge of the final-state

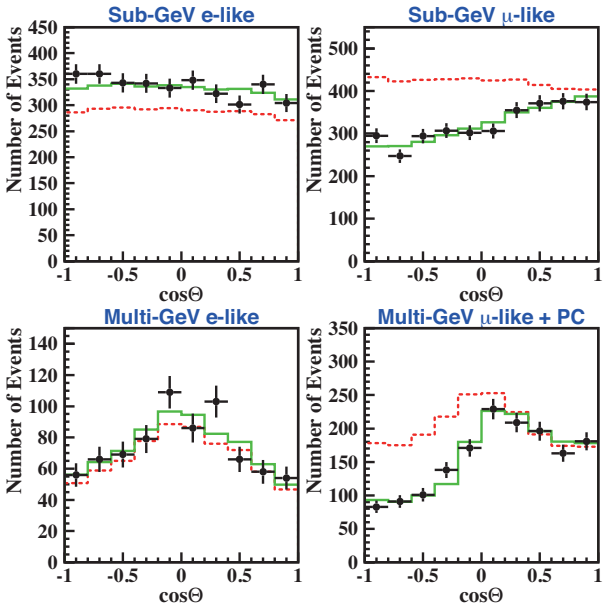

Figure 13.6: The zenith angle distributions for fully contained 1-ring e-like and μ-like events with visible energy < 1.33 GeV (sub-GeV) and > 1.33 GeV (multi-GeV). For multi-GeV μ-like events, a combined distribution with partially contained (PC) events is shown. The dotted histograms show the non-oscillated Monte Carlo events, and the solid histograms show the best-fit expectations for $\nu_\mu \leftrightarrow \nu_\tau$ oscillations. (This figure is provided by the Super-Kamiokande Collaboration.)

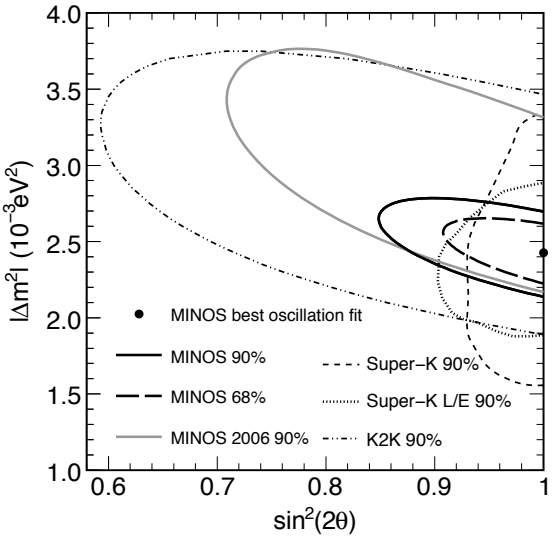

Figure 13.7: Allowed region for the $\nu_\mu \leftrightarrow \nu_\tau$ oscillation parameters from the MINOS results published in 2008. The 68 % and 90 % CL allowed regions are shown together with the SK-I and K2K 90 % CL allowed regions. This figure is taken from Ref. 22.

leptons, and therefore neutrino and antineutrino induced events cannot be discriminated. Neutrino events having their vertex in the 22.5 kton fiducial volume in Super-Kamiokande are classified into fully contained (FC) events and partially contained (PC) events. The FC events are required to have no activity in the anti-counter. The total visible energy (proportional to the total number of photoelectrons measured by the photomultiplier tubes in the inner detector) can be measured for the FC events.

FC events are subjected to particle identification of the final-state particles. Single-ring events have only one charged lepton which radiates Chrenkov light in the final state, and particle identification is particularly clean for single-ring FC events. The method adopted for the FC events identifies the particle types as e-like or μ-like based on the pattern of each Cherenkov ring. A ring produced by an e-like ($e^\pm$, γ) particle exhibits a more diffuse pattern than that produced by a μ-like ($\mu^\pm$, $\pi^\pm$) particle, since an e-like particle produces an electromagnetic shower and low-energy electrons suffer considerable multiple Coulomb scattering in water. All the PC events were assumed to be μ-like since the PC events comprise a 98% pure charged-current ν_μ sample.

Fig. 13.6 shows the zenith-angle distributions of e-like and μ-like events from the SK-I measurement [102]. $\cos\theta = 1$ corresponds to the downward direction, while $\cos\theta = -1$ corresponds to the upward direction. Events included in these plots are single-ring FC events subdivided into sub-GeV (visible energy < 1.33 GeV) events and multi-GeV (visible energy > 1.33 GeV) events. Note that the zenith-angle distribution of the multi-GeV μ-like events is shown combined with that of the PC events. The final-state leptons in these events have good directional correlation with the parent neutrinos. The dotted histograms show the Monte Carlo expectation for neutrino events. If the produced flux of atmospheric neutrinos of a given flavour remains unchanged at the detector, the data should have similar distributions to the expectation. However, the zenith-angle distribution of the μ-like events shows a strong deviation from the expectation. On the other hand, the zenith-angle distribution of the e-like events is consistent with the expectation. This characteristic feature may be interpreted that muon neutrinos coming from the opposite side of the Earth's atmosphere, having travelled $\sim 10,000$ km, oscillate into other neutrinos and disappeared, while oscillations still do not take place for muon neutrinos coming from above the detector, having travelled a few km. Disappeared muon neutrinos may have oscillated into tau neutrinos because there is no indication of electron neutrino appearance. The atmospheric neutrinos corresponding to the events shown in Fig. 13.6 have $E = 1 \sim 10$ GeV. With $L = 10000$ km, the hypothesis of neutrino oscillations suggests $\Delta m^2 \sim 10^{-3} - 10^{-4}$ eV^2. The solid histograms show the best-fit results of a two-neutrino oscillation analysis with the hypothesis of $\nu_\mu \leftrightarrow \nu_\tau$. (To constrain the flux of atmospheric neutrinos through the accurately predicted ν_μ/ν_e ratio, e-like events are included in the fit.) They reproduce the observed data well. The oscillation parameters determined by the SK-I atmospheric neutrino data are $\sin^2 2\theta_{\rm A} > 0.92$ and $1.5 \times 10^{-3} < |\Delta m^2_{\rm A}| < 3.4 \times 10^{-3}$ eV^2 at 90% confidence level. For the allowed parameter region, see Fig. 13.7.

Though the SK-I atmospheric neutrino observations gave compelling evidence for muon neutrino disappearance which is consistent with two-neutrino oscillation $\nu_\mu \leftrightarrow \nu_\tau$ [103], the question may be asked whether the observed muon neutrino disappearance is really due to neutrino oscillations. First, other exotic explanations such as neutrino decay [104] and quantum decoherence [105] cannot be completely ruled out from the zenith-angle distributions alone. To provide firm evidence for neutrino oscillation, we need to confirm the characteristic sinusoidal behavior of the conversion probability as a function of neutrino energy E for a fixed distance L in the case of long-baseline neutrino oscillation experiments, or as a function of L/E in the case of atmospheric neutrino experiments. By selecting events with high L/E resolution, evidence for the dip in the L/E distribution was observed at the right place expected from the interpretation of the SK-I data in terms of $\nu_\mu \leftrightarrow \nu_\tau$ oscillations [14], Fig. 13.8. This dip cannot be explained by alternative hypotheses of neutrino decay and neutrino decoherence, and they are excluded at more than 3σ in comparison with the neutrino oscillation interpretation. At 90% CL, the constraints obtained from the L/E analysis are $1.9 \times 10^{-3} < |\Delta m^2_{\rm A}| < 3.0 \times 10^{-3}$ eV^2 and $\sin^2 2\theta_{\rm A} > 0.90$. (see Fig. 13.7).

Second, a natural question is whether appearance of tau neutrinos has been observed in the Super-Kamiokande detector. Detection of ν_τ CC reactions in a water Cherenkov detector is not easy. In addition to the low flux of atmospheric neutrinos above the threshold of these reactions, 3.5 GeV, the interactions are mostly deep inelastic scattering, leading to complicated multiring event pattern. Nevertheless, search for a ν_τ appearance signal by using criteria to enhance ν_τ CC events (high visible energy, high average multiplicity, etc.) found candidate

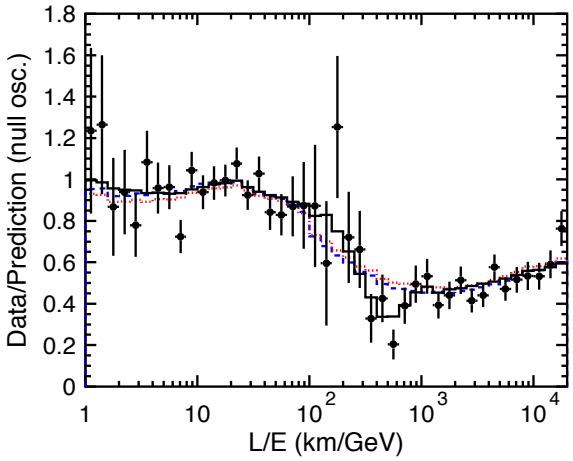

Figure 13.8: Results of the L/E analysis of SK-I atmospheric neutrino data. The points show the ratio of the data to the Monte Carlo prediction without oscillations, as a function of the reconstructed L/E. The error bars are statistical only. The solid line shows the best fit with 2-flavour $\nu_\mu \leftrightarrow \nu_\tau$ oscillations. The dashed and dotted lines show the best fit expectations for neutrino decay and neutrino decoherence hypotheses, respectively. (From Ref. 14.)

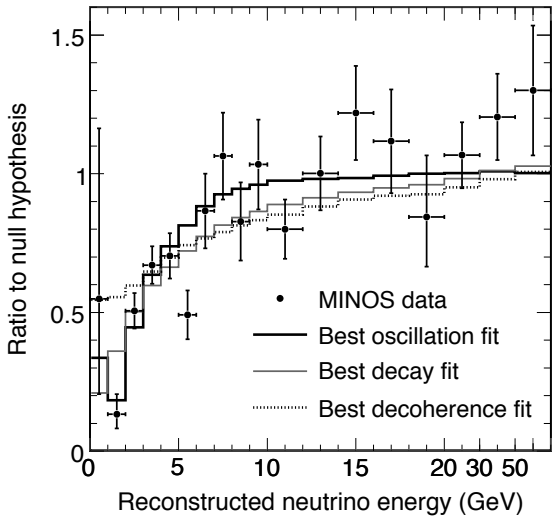

Figure 13.9: Ratio of the MINOS far detector data and the expected spectrum for no oscillations. The best-fit with the hypothesis of $\nu_\mu \to \nu_\tau$ oscillations as well as the best fit to alternative models (neutrino decay and decoherence) is also shown. This figure is taken from Ref. 22.

events in the upward-going direction as expected [103]. However, the significance of the signal is yet marginal; no ν_τ appearance hypothesis is disfavored at only 2.4σ.

13.5.2. *Results from accelerator experiments* :

The $\Delta m^2 \geq 2 \times 10^{-3}$ eV^2 region can be explored by accelerator-based long-baseline experiments with typically $E \sim 1$ GeV and $L \sim$ several hundred km. With a fixed baseline distance and a narrower, well understood neutrino spectrum, the value of $|\Delta m^2_{\rm A}|$ and, with higher statistics, also the mixing angle, are potentially better constrained in accelerator experiments than from atmospheric neutrino observations.

The K2K (KEK-to-Kamioka) long-baseline neutrino oscillation experiment [20] is the first accelerator-based experiment with a neutrino path length extending hundreds of kilometers. K2K aimed at confirmation of the neutrino oscillation in ν_μ disappearance in the $|\Delta m^2_{\rm A}| \geq 2 \times 10^{-3}$ eV^2 region. A horn-focused wide-band muon neutrino beam having an average $L/E_\nu \sim 200$ ($L = 250$ km, $\langle E_\nu \rangle \sim 1.3$ GeV), was produced by 12-GeV protons from the KEK-PS and directed to the Super-Kamiokande detector. The spectrum and profile of the neutrino beam were measured by a near neutrino detector system located 300 m downstream from the production target.

The construction of the K2K neutrino beam line and the near detector began before Super-Kamiokande's discovery of atmospheric neutrino oscillations, and the stable data-taking started in June 1999. Super-Kamiokande events caused by accelerator-produced neutrinos were selected using the timing information from the global positioning system. Data were intermittently taken until November 2004. The total number of protons on target (POT) for physics analysis amounted to 0.92×10^{20}. The observed number of beam-originated FC events in the 22.5 kton fiducial volume of Super-Kamiokande was 112, compared with an expectation of $158.1^{+9.2}_{-8.6}$ events without oscillation. For 58 1-ring μ-like subset of the data, the neutrino energy was reconstructed from measured muon momentum and angle, assuming CC quasielestic kinematics. The measured energy spectrum showed the distortion expected from neutrino oscillations. From a 2-flavour neutrino oscillation analysis, the allowed parameter region shown in Fig. 13.7 is obtained. At $\sin^2 2\theta_{\rm A} = 1.0$, $1.9 \times 10^{-3} < |\Delta m^2_{\rm A}| < 3.5 \times 10^{-3}$ eV^2 at the 90% CL with the best-fit value of 2.8×10^{-3} eV^2. The probability that the observations are due to a statistical fluctuation instead of neutrino oscillation is 0.0015% or 4.3 σ [20].

MINOS is the second long-baseline neutrino oscillation experiment with near and far detectors. Neutrinos are produced by the NuMI (Neutrinos at the Main Injector) facility using 120 GeV protons from the Fermilab Main Injector. The far detector is a 5.4 kton (total mass) iron-scintillator tracking calorimeter with toroidal magnetic field, located underground in the Soudan mine. The baseline distance is 735 km. The near detector is also an iron-scintillator tracking calorimeter with toroidal magnetic field, with a total mass of 0.98 kton. The neutrino beam is a horn-focused wide-band beam. Its energy spectrum can be varied by moving the target position relative to the first horn and changing the horn current.

MINOS started the neutrino-beam run in 2005. Initial results were reported [21] using tha data taken between May 2005 and February 2006 with 1.27×10^{20} POT, and the updated results corresponding to a total POT of 3.36×10^{20} (May 2005 to July 2007) were published [22] recently. During this period, a "low-energy" option was mostly chosen for the spectrum of the neutrino beam so that the flux was enhanced in the 1-5 GeV energy range. In the far detector, a total of 848 CC events were produced by the NuMI beam, compared to the unoscillated expectation of 1065 ± 60 (syst) events. Fig. 13.9 shows the ratio of observed energy spectrum and the expected one with no oscillation. Fig. 13.7 shows the 68% and 90% CL allowed regions obtained from the $\nu_\mu \to \nu_\tau$ oscillation analysis. The results are compared with the 90% CL allowed regions obtained from the initial MINOS [21], SK-I zenith-angle dependence [102], the SK-I L/E analysis [14], and the K2K results [20]. The MINOS results are consistent with the SK-I and K2K results, and constrain the oscillation parameters as $|\Delta m^2_{\rm A}| = (2.43 \pm 0.13) \times 10^{-3}$ eV^2 (68% CL) and $\sin^2 2\theta_{\rm A} > 0.90$ at 90% CL. The alternative models to explain the ν_μ disappearance, neutrino decay and quantum decoherence of neutrinos, are disfavored at the 3.7 and 5.7σ, respectively, by the MINOS data (see Fig. 13.9).

The regions of neutrino parameter space favoured or excluded by various neutrino oscillation experiments are shown in Fig. 13.10.

A promising method to confirm the appearance of ν_τ from $\nu_\mu \to \nu_\tau$ oscillations is an accelerator long-baseline experiment using emulsion technique to identify short-lived τ leptons event-by-event. The only experiment of this kind is OPERA [106] with a neutrino source at CERN and a detector at Gran Sasso with the baseline distance of 732 km. The detector is a combination of the "Emulsion Cloud Chamber" and magnetized spectrometer. The CNGS (CERN Neutrinos to Gran Sasso) neutrino beam with $\langle E_\nu \rangle = 17$ GeV is produced by high-energy protons from the CERN SPS. With so-called shared SPS operation, 4.5×10^{19} POT/yr is expected. With this beam and 1.35 kt target mass, a ν_τ appearance signal of about 10 events is expected in 5 years run with full intensity.

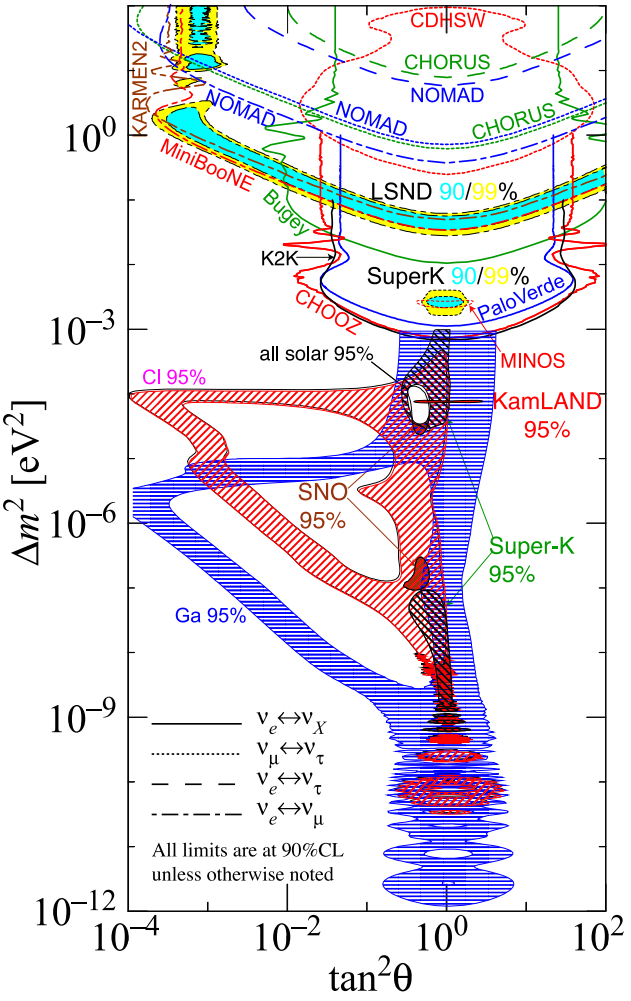

Figure 13.10: The regions of squared-mass splitting and mixing angle favored or excluded by various experiments. The figure was contributed by H. Murayama (University of California, Berkeley, and IPMU, University of Tokyo). References to the data used in the figure can be found at `http://hitoshi.berkeley.edu/neutrino`.

13.6. Measurements of θ_{13}

Reactor $\bar{\nu}_e$ disappearance experiments with $L \sim 1$ km, $\langle E \rangle \sim 3$ MeV are sensitive to $\sim E/L \sim 3\times10^{-3}$ eV$^2 \sim |\Delta m^2_{\rm A}|$. At this baseline distance, the reactor $\bar{\nu}_e$ oscillations driven by $\Delta m^2_\odot$ are negligible. Therefore, as can be seen from Eq. (13.22) and Eq. (13.24), θ_{13} can be directly measured. A reactor neutrino oscillation experiment at the Chooz nuclear power station in France [107] was the first experiment of this kind. The detector was located in an underground laboratory with 300 mwe (meter water equivalent) rock overburden, at about 1 km from the neutrino source. It consisted of a central 5-ton target filled with 0.09% gadolinium loaded liquid scintillator, surrounded by an intermediate 17-ton and outer 90-ton regions filled with undoped liquid scintillator. Reactor $\bar{\nu}_e$'s were detected via the reaction $\bar{\nu}_e + p \to e^+ + n$. Gd-doping was chosen to maximize the neutron capture efficiency. The CHOOZ experiment [107] found no evidence for $\bar{\nu}_e$ disappearance. The 90% CL upper limit for $\Delta m^2 = 2.0 \times 10^{-3}$ eV^2 is $\sin^2 2\theta_{13} < 0.19$ and for the MINOS measurement [22] of $|\Delta m^2_{\rm A}| = 2.43 \times 10^{-3}$ eV, $\sin^2 2\theta_{13} < 0.15$, both at 90% CL.

A similar reactor neutrino oscillation experiment was also conducted at the Palo Verde Nuclear Generating Station in Arizona [108]. This experiment used a segmented Gd-loaded liquid scintillator detector with a total mass of 11.34 tons. The detector was located at a shallow underground site with only 32 mwe. This experiment found no evidence for $\bar{\nu}_e$ disappearance either [108]. The excluded oscillation parameter region is consistent with, but less restrictive than, the CHOOZ results.

In the accelerator neutrino oscillation experiments with conventional neutrino beams, θ_{13} can be measured using $\nu_\mu \to \nu_e$ appearance. The K2K experiment searched for the $\nu_\mu \to \nu_e$ appearance signal [109], but no evidence was found. Using the dominant term in the probability of $\nu_\mu \to \nu_e$ appearance (see Eq. (13.23) and Eq. (13.24)),

$$P(\nu_\mu \to \nu_e) = \sin^2 2\theta_{13} \cdot \sin^2\theta_{23} \cdot \sin^2(1.27\Delta m^2 L/E) \sim \frac{1}{2}\sin^2 2\theta_{13} \sin^2(1.27\Delta m^2 L/E)\,, \qquad (13.75)$$

the 90% CL upper limit $\sin^2 2\theta_{13} < 0.26$ was obtained at the K2K measurement of $\Delta m^2 = 2.8 \times 10^{-3}$ eV^2. Though this limit is less significant than the CHOOZ limit, it is the first result obtained from an accelerator ν_e appearance experiment.

By examining the exact expression for the oscillation probability, however, it is understood that some of the neglected terms could have rather large effects and the unknown CP-violating phase δ causes uncertainties in determining the value of θ_{13}. Actually, from the measurement of $\nu_\mu \to \nu_e$ appearance, θ_{13} is given as a function of δ for a given sign of Δm^2_{32}. Also, deviations from maximal θ_{23} mixing would cause a further uncertainty. Therefore, a single experiment with a neutrino beam cannot determine the value of θ_{13} though it is possible to establish non-zero θ_{13}.

Turning to atmospheric and solar neutrino observations, Eq. (13.40) to Eq. (13.43) and Eq. (13.62) indicate that they are sensitive to θ_{13} through sub-leading effects. So far the SK group analyzed its atmospheric neutrino data [64] and the SNO group analyzed [97] the data from all solar neutrino experiments, with or without the KamLAND data, in terms of 3-neutrino oscillations.

The SK-I atmospheric neutrino data were analyzed in the three-neutrino oscillation framework with the approximation of one mass scale dominance ($\Delta m^2_\odot = 0$) [64]. Since the matter effects in $\nu_e \leftrightarrow \nu_{\mu,\tau}$ oscillations cause differences for the normal and inverted mass hierarchy cases, both cases were analyzed. For the $\Delta m^2_{\rm A} > 0$ case, $\sin^2\theta_{13} < 0.14$ and $0.37 < \sin^2\theta_{23} < 0.65$ was obtained at 90% CL, while for the $\Delta m^2_{\rm A} < 0$ case, weaker constraints, $\sin^2\theta_{13} < 0.27$ and $0.37 < \sin^2\theta_{23} < 0.69$ were obtained at 90% CL.

The recent SNO's three-neutrino oscillation analysis using its Phase I and Phase II joint analysis [97] results and the results from all other solar neutrino experiments and the KamLAND experiment has yielded the best fit value of $\sin^2\theta_{13} = 2.00^{+2.09}_{-1.63} \times 10^{-2}$ [97]. At the 95% CL, this result implies $\sin^2\theta_{13} < 0.057$ [97].

Finally, it should be noted that a global analysis [110] of all available neutrino oscillation data gave a hint of non-zero $\sin^2\theta_{13}$; $\sin^2\theta_{13} = 0.016 \pm 0.010$ at 1σ CL.

13.7. The three neutrino mixing

All existing compelling data on neutrino oscillations can be described assuming 3-flavour neutrino mixing in vacuum. This is the minimal neutrino mixing scheme which can account for the currently available data on the oscillations of the solar (ν_e), atmospheric (ν_μ and $\bar{\nu}_\mu$), reactor ($\bar{\nu}_e$) and accelerator (ν_μ) neutrinos. The (left-handed) fields of the flavour neutrinos ν_e, ν_μ and ν_τ in the expression for the weak charged lepton current in the CC weak interaction Lagrangian, are linear combinations of the LH components of the fields of three massive neutrinos ν_j:

$$\mathcal{L}_{\rm CC} = -\frac{g}{\sqrt{2}} \sum_{l=e,\mu,\tau} \overline{l_L}(x)\,\gamma_\alpha\,\nu_{lL}(x)\,W^{\alpha\dagger}(x) + h.c.\,,$$

$$\nu_{l\rm L}(x) = \sum_{j=1}^{3} U_{lj}\,\nu_{j\rm L}(x), \qquad (13.76)$$

where U is the 3×3 unitary neutrino mixing matrix [17,18]. The mixing matrix U can be parameterized by 3 angles, and, depending on

whether the massive neutrinos ν_j are Dirac or Majorana particles, by 1 or 3 CP violation phases [30,31]:

$$U = \begin{bmatrix} c_{12}c_{13} & s_{12}c_{13} & s_{13}e^{-i\delta} \\ -s_{12}c_{23} - c_{12}s_{23}s_{13}e^{i\delta} & c_{12}c_{23} - s_{12}s_{23}s_{13}e^{i\delta} & s_{23}c_{13} \\ s_{12}s_{23} - c_{12}c_{23}s_{13}e^{i\delta} & -c_{12}s_{23} - s_{12}c_{23}s_{13}e^{i\delta} & c_{23}c_{13} \end{bmatrix} \times \mathrm{diag}(1,\ e^{i\frac{\alpha_{21}}{2}},\ e^{i\frac{\alpha_{31}}{2}})\ . \quad (13.77)$$

where $c_{ij} = \cos\theta_{ij}$, $s_{ij} = \sin\theta_{ij}$, the angles $\theta_{ij} = [0, \pi/2]$, $\delta = [0, 2\pi]$ is the Dirac CP violation phase and α_{21}, α_{31} are two Majorana CP violation phases. Thus, in the case of massive Dirac neutrinos, the neutrino mixing matrix U is similar, in what concerns the number of mixing angles and CP violation phases, to the CKM quark mixing matrix. The presence of two additional physical CP violation phases in U if ν_j are Majorana particles is a consequence of the special properties of the latter (see, *e.g.*, [29,30]) .

As we see, the fundamental parameters characterizing the 3-neutrino mixing are: i) the 3 angles θ_{12}, θ_{23}, θ_{13}, ii) depending on the nature of massive neutrinos ν_j - 1 Dirac (δ), or 1 Dirac + 2 Majorana ($\delta, \alpha_{21}, \alpha_{31}$), CP violation phases, and iii) the 3 neutrino masses, m_1, m_2, m_3. Thus, depending on whether the massive neutrinos are Dirac or Majorana particles, this makes 7 or 9 additional parameters in the "Standard" Model of particle interactions.

The neutrino oscillation probabilities depend (Section 13.2), in general, on the neutrino energy, E, the source-detector distance L, on the elements of U and, for relativistic neutrinos used in all neutrino experiments performed so far, on $\Delta m^2_{ij} \equiv (m^2_i - m^2_j)$, $i \neq j$. In the case of 3-neutrino mixing there are only two independent neutrino mass squared differences, say $\Delta m^2_{21} \neq 0$ and $\Delta m^2_{31} \neq 0$. The numbering of massive neutrinos ν_j is arbitrary. It proves convenient from the point of view of relating the mixing angles θ_{12}, θ_{23} and θ_{13} to observables, to identify $|\Delta m^2_{21}|$ with the smaller of the two neutrino mass squared differences, which, as it follows from the data, is responsible for the solar ν_e and, the observed by KamLAND, reactor $\bar{\nu}_e$ oscillations. We will number (just for convenience) the massive neutrinos in such a way that $m_1 < m_2$, so that $\Delta m^2_{21} > 0$. With these choices made, there are two possibilities: either $m_1 < m_2 < m_3$, or $m_3 < m_1 < m_2$. Then the larger neutrino mass square difference $|\Delta m^2_{31}|$ or $|\Delta m^2_{32}|$, can be associated with the experimentally observed oscillations of the atmospheric ν_μ and $\bar{\nu}_\mu$ and accelerator ν_μ. The effects of Δm^2_{31} or Δm^2_{32} in the oscillations of solar ν_e, and of Δm^2_{21} in the oscillations of atmospheric ν_μ and $\bar{\nu}_\mu$ and of accelerator ν_μ, are relatively small and subdominant as a consequence of the facts that i) L, E and L/E in the experiments with solar ν_e and with atmospheric ν_μ and $\bar{\nu}_\mu$ or accelerator ν_μ, are very different, ii) the conditions of production and propagation (on the way to the detector) of the solar ν_e and of the atmospheric ν_μ and $\bar{\nu}_\mu$ or accelerator ν_μ, are very different, and iii) $|\Delta m^2_{21}|$ and $|\Delta m^2_{31}|$ ($|\Delta m^2_{32}|$) in the case of $m_1 < m_2 < m_3$ ($m_3 < m_1 < m_2$), as it follows from the data, differ by approximately a factor of 30, $|\Delta m^2_{21}| \ll |\Delta m^2_{31(32)}|$, $|\Delta m^2_{21}|/|\Delta m^2_{31(32)}| \cong 0.03$. This implies that in both cases of $m_1 < m_2 < m_3$ and $m_3 < m_1 < m_2$ we have $\Delta m^2_{32} \cong \Delta m^2_{31}$ with $|\Delta m^2_{31} - \Delta m^2_{32}| = |\Delta m^2_{21}| \ll |\Delta m^2_{31,32}|$.

It follows from the results of CHOOZ and Palo Verde experiments with reactor $\bar{\nu}_e$ [107,108] that, in the convention we use, in which $0 < \Delta m^2_{21} < |\Delta m^2_{31(32)}|$, the element $|U_{e3}| = \sin\theta_{13}$ of the neutrino mixing matrix U is small (we will quantify this statement below). This makes it possible to identify the angles θ_{12} and θ_{23} as the neutrino mixing angles associated with the solar ν_e and the dominant atmospheric ν_μ (and $\bar{\nu}_\mu$) oscillations, respectively. The angles θ_{12} and θ_{23} are often called "solar" and "atmospheric" neutrino mixing angles, and are often denoted as $\theta_{12} = \theta_\odot$ and $\theta_{23} = \theta_{\rm A}$ (or $\theta_{\rm atm}$) while Δm^2_{21} and Δm^2_{31} are often referred to as the "solar" and "atmospheric" neutrino mass squared differences and are often denoted as $\Delta m^2_{21} \equiv \Delta m^2_\odot$, $\Delta m^2_{31} \equiv \Delta m^2_{\rm A}$ (or $\Delta m^2_{\rm atm}$).

The solar neutrino data tell us that $\Delta m^2_{21} \cos 2\theta_{12} > 0$. In the convention employed by us we have $\Delta m^2_{21} > 0$. Correspondingly, in this convention one must have $\cos 2\theta_{12} > 0$.

The existing neutrino oscillation data allow us to determine the parameters which drive the solar neutrino and the dominant atmospheric neutrino oscillations, $\Delta m^2_\odot = \Delta m^2_{21}$, θ_{12}, and $|\Delta m^2_{\rm A}| = |\Delta m^2_{31}| \cong |\Delta m^2_{32}|$, θ_{23}, with a relatively good precision, and to obtain rather stringent limits on the angle θ_{13} [107,108]. The best fit values and the 99.73% C.L. allowed ranges of Δm^2_{21}, $\sin^2\theta_{12}$, $|\Delta m^2_{31(32)}|$ and $\sin^2\theta_{23}$, read [111,112]:

$$(\Delta m^2_{21})_{\rm BF} = 7.65 \times 10^{-5}\ \ \mathrm{eV}^2,$$
$$7.05 \times 10^{-5}\ \ \mathrm{eV}^2 \leq \Delta m^2_{21} \leq 8.34 \times 10^{-5}\ \ \mathrm{eV}^2, \quad (13.78)$$

$$(\sin^2\theta_{12})_{\rm BF} = 0.304, \qquad 0.25 \leq \sin^2\theta_{12} \leq 0.37\,, \quad (13.79)$$

$$(|\Delta m^2_{31}|)_{\rm BF} = 2.40 \times 10^{-3}\ \ \mathrm{eV}^2,$$
$$2.07 \times 10^{-3}\ \ \mathrm{eV}^2 \leq |\Delta m^2_{31}| \leq 2.75 \times 10^{-3}\ \ \mathrm{eV}^2, \quad (13.80)$$

$$(\sin^2\theta_{23})_{\rm BF} = 0.5, \qquad 0.36 \leq \sin^2\theta_{23} \leq 0.67\,. \quad (13.81)$$

The existing SK atmospheric neutrino, K2K and MINOS data do not allow to determine the sign of $\Delta m^2_{31(32)}$. Maximal solar neutrino mixing, *i.e.*, $\theta_{12} = \pi/4$, is ruled out at more than 6σ by the data. Correspondingly, one has $\cos 2\theta_{12} \geq 0.26$ (at 99.73% C.L.). A stringent upper limit on the angle θ_{13} was provided by the CHOOZ experiment with reactor $\bar{\nu}_e$ [107]: at $|\Delta m^2_{31}| \cong 2.4 \times 10^{-3}$ eV^2 the limit reads

$$\sin^2 2\theta_{13} < 0.15 \quad \text{at } 90\% \text{ C.L.} \quad (13.82)$$

A combined 3-neutrino oscillation analysis of the global data gives [112]:

$$\sin^2\theta_{13} < 0.035\ (0.056) \quad \text{at } 90\%\ (99.73\%)\ \text{C.L.} \quad (13.83)$$

These results imply that $\theta_{23} \cong \pi/4$, $\theta_{12} \cong \pi/5.4$ and that $\theta_{13} < \pi/13$. Correspondingly, the pattern of neutrino mixing is drastically different from the pattern of quark mixing.

At present no experimental information on the Dirac and Majorana CP violation phases in the neutrino mixing matrix is available. Thus, the status of CP symmetry in the lepton sector is unknown. If $\theta_{13} \neq 0$, the Dirac phase δ can generate CP violation effects in neutrino oscillations [30,42,43]. The magnitude of CP violation in $\nu_l \to \nu_{l'}$ and $\bar{\nu}_l \to \bar{\nu}_{l'}$ oscillations, $l \neq l' = e, \mu, \tau$, is determined, as we have seen, by the rephasing invariant J_{CP} (see Eq. (13.19)), which in the "standard" parametrisation of the neutrino mixing matrix (Eq. (13.77)) has the form:

$$J_{CP} \equiv \mathrm{Im}\,(U_{\mu 3}\, U^*_{e3}\, U_{e2}\, U^*_{\mu 2}) = \frac{1}{8}\cos\theta_{13} \sin 2\theta_{12}\ \sin 2\theta_{23}\ \sin 2\theta_{13}\ \sin\delta\,. \quad (13.84)$$

Thus, the size of CP violation effects in neutrino oscillations depends on the magnitude of the currently unknown values of the "small" angle θ_{13} and the Dirac phase δ.

As we have indicated, the existing data do not allow one to determine the sign of $\Delta m^2_{\rm A} = \Delta m^2_{31(2)}$. In the case of 3-neutrino mixing, the two possible signs of $\Delta m^2_{31(2)}$ correspond to two types of neutrino mass spectrum. In the widely used conventions of numbering the neutrinos with definite mass in the two cases, the two spectra read: *i) spectrum with normal ordering*: $m_1 < m_2 < m_3$, $\Delta m^2_{\rm A} = \Delta m^2_{31} > 0$, $\Delta m^2_\odot \equiv \Delta m^2_{21} > 0$, $m_{2(3)} = (m^2_1 + \Delta m^2_{21(31)})^{\frac{1}{2}}$; *ii) spectrum with inverted ordering (IO)*: $m_3 < m_1 < m_2$, $\Delta m^2_{\rm A} = \Delta m^2_{32} < 0$, $\Delta m^2_\odot \equiv \Delta m^2_{21} > 0$, $m_2 = (m^2_3 + \Delta m^2_{23})^{\frac{1}{2}}$, $m_1 = (m^2_3 + \Delta m^2_{23} - \Delta m^2_{21})^{\frac{1}{2}}$.
Depending on the values of the lightest neutrino mass [113], $\min(m_j)$, the neutrino mass spectrum can also be:

– *Normal Hierarchical (NH)*: $m_1 \ll m_2 < m_3$, $m_2 \cong (\Delta m^2_\odot)^{\frac{1}{2}}$, $m_3 \cong |\Delta m^2_{\rm A}|^{\frac{1}{2}}$; or

– *Inverted Hierarchical (IH)*: $m_3 \ll m_1 < m_2$, with $m_{1,2} \cong |\Delta m^2_{\rm A}|^{\frac{1}{2}} \sim 0.05$ eV; or

– *Quasi-Degenerate (QD)*: $m_1 \cong m_2 \cong m_3 \cong m_0$, $m^2_j \gg |\Delta m^2_{\rm A}|$, $m_0 \gtrsim 0.10$ eV.

All three types of spectrum are compatible with the existing constraints on the absolute scale of neutrino masses m_j. Information about the latter can be obtained, *e.g.*, by measuring the spectrum of electrons near the end point in ^{3}H β-decay experiments [115–117] and from cosmological and astrophysical data. The most stringent upper bounds on the $\bar{\nu}_e$ mass were obtained in the Troitzk [116] and Mainz [117] experiments:

$$m_{\bar{\nu}_e} < 2.3 \text{ eV} \quad \text{at } 95\% \text{ C.L.} \tag{13.85}$$

We have $m_{\bar{\nu}_e} \cong m_{1,2,3}$ in the case of QD spectrum. The KATRIN experiment [117] is planned to reach sensitivity of $m_{\bar{\nu}_e} \sim 0.20$ eV, *i.e.*, it will probe the region of the QD spectrum.

The Cosmic Microwave Background (CMB) data of the WMAP experiment, combined with supernovae data and data on galaxy clustering can be used to obtain an upper limit on the sum of neutrinos masses [118] (see review on Cosmological Parameters): $\sum_j m_j \lesssim 0.68$ eV, 95% C.L. A more conservative estimate of the uncertainties in the astrophysical data leads to a somewhat weaker constraint (see *e.g.*, Ref. 119): $\sum_j m_j \lesssim 1.7$ eV, 95% C.L.

It follows from these data that neutrino masses are much smaller than the masses of charged leptons and quarks. If we take as an indicative upper limit $m_j \lesssim 0.5$ eV, we have $m_j/m_{l,q} \lesssim 10^{-6}$, $l = e, \mu, \tau$, $q = d, s, b, u, c, t$. It is natural to suppose that the remarkable smallness of neutrino masses is related to the existence of a new fundamental mass scale in particle physics, and thus to new physics beyond that predicted by the Standard Model.

13.7.1. *The see-saw mechanism and the baryon asymmetry of the Universe* :

A natural explanation of the smallness of neutrino masses is provided by the see-saw mechanism of neutrino mass generation [3]. An integral part of the simplest version of this mechanism - the so-called "type I see-saw", are the RH neutrinos ν_{lR} (RH neutrino fields $\nu_{lR}(x)$). The latter are assumed to possess a Majorana mass term as well as Yukawa type coupling $\mathcal{L}_{\rm Y}(x)$ with the Standard Model lepton and Higgs doublets, $\psi_{lL}(x)$ and $\Phi(x)$, respectively, $(\psi_{lL}(x))^T = (\nu_{lL}^T(x) \quad l_L^T(x))$, $l = e, \mu, \tau$, $(\Phi(x))^T = (\Phi^{(0)} \ \Phi^{(-)})$. In the basis in which the Majorana mass matrix of RH neutrinos is diagonal, we have:

$$\mathcal{L}_{\rm Y,M}(x) = \left(\lambda_{il}\, \overline{N_{iR}}(x)\, \Phi^\dagger(x)\, \psi_{lL}(x) + \text{h.c.}\right) - \frac{1}{2}\, M_i\, \overline{N_i}(x)\, N_i(x)\,, \tag{13.86}$$

where λ_{il} is the matrix of neutrino Yukawa couplings and N_i ($N_i(x)$) is the heavy RH Majorana neutrino (field) possessing a mass $M_i > 0$. When the electroweak symmetry is broken spontaneously, the neutrino Yukawa coupling generates a Dirac mass term: $m^D_{il}\, \overline{N_{iR}}(x)\, \nu_{lL}(x) + \text{h.c.}$, with $m^D = v\lambda$, $v = 174$ GeV being the Higgs doublet v.e.v. In the case when the elements of m^D are much smaller than M_k, $|m^D_{il}| \ll M_k$, $i, k = 1, 2, 3$, $l = e, \mu, \tau$, the interplay between the Dirac mass term and the mass term of the heavy (RH) Majorana neutrinos N_i generates an effective Majorana mass (term) for the LH flavour neutrinos [3]: $m^{LL}_{l'l} \cong -(m^D)^T_{l'j} M_j^{-1} m^D_{jl}$. In grand unified theories, m^D is typically of the order of the charged fermion masses. In $SO(10)$ theories, for instance, m^D coincides with the up-quark mass matrix. Taking indicatively $m^{LL} \sim 0.1$ eV, $m^D \sim 100$ GeV, one finds $M \sim 10^{14}$ GeV, which is close to the scale of unification of the electroweak and strong interactions, $M_{GUT} \cong 2 \times 10^{16}$ GeV. In GUT theories with RH neutrinos one finds that indeed the heavy Majorana neutrinos N_j naturally obtain masses which are by few to several orders of magnitude smaller than M_{GUT}. Thus, the enormous disparity between the neutrino and charged fermion masses is explained in this approach by the huge difference between effectively the electroweak symmetry breaking scale and M_{GUT}.

An additional attractive feature of the see-saw scenario is that the generation and smallness of neutrino masses is related via the leptogenesis mechanism [2] to the generation of the baryon asymmetry of the Universe. The Yukawa coupling in Eq. (13.86), in general, is not CP conserving. Due to this CP-nonconserving coupling the heavy Majorana neutrinos undergo, *e.g.*, the decays $N_j \to l^+ + \Phi^{(-)}$, $N_j \to l^- + \Phi^{(+)}$, which have different rates: $\Gamma(N_j \to l^+ + \Phi^{(-)}) \neq \Gamma(N_j \to l^- + \Phi^{(+)})$. When these decays occur in the Early Universe at temperatures somewhat below the mass of, say, N_1, so that the latter are out of equilibrium with the rest of the particles present at that epoch, CP violating asymmetries in the individual lepton charges L_l, and in the total lepton charge L, of the Universe are generated. These lepton asymmetries are converted into a baryon asymmetry by $(B - L)$ conserving, but $(B + L)$ violating, sphaleron processes, which exist in the Standard Model and are effective at temperatures $T \sim (100 - 10^{12})$ GeV. If the heavy neutrinos N_j have hierarchical spectrum, $M_1 \ll M_2 \ll M_3$, the observed baryon asymmetry can be reproduced provided the mass of the lightest one satisfies $M_1 \gtrsim 10^9$ GeV [120]. Thus, in this scenario, the neutrino masses and mixing and the baryon asymmetry have the same origin - the neutrino Yukawa couplings and the existence of (at least two) heavy Majorana neutrinos. Moreover, quantitative studies based on recent advances in leptogenesis theory [121] have shown that the Dirac and/or Majorana phases in the neutrino mixing matrix U can provide the CP violation, necessary in leptogenesis for the generation of the observed baryon asymmetry of the Universe [122]. This implies, in particular, that if the CP symmetry is established not to hold in the lepton sector due to U, at least some fraction (if not all) of the observed baryon asymmetry might be due to the Dirac and/or Majorana CP violation present in the neutrino mixing.

13.7.2. *The nature of massive neutrinos* :

The experiments studying flavour neutrino oscillations cannot provide information on the nature - Dirac or Majorana, of massive neutrinos [30,44]. Establishing whether the neutrinos with definite mass ν_j are Dirac fermions possessing distinct antiparticles, or Majorana fermions, i.e. spin 1/2 particles that are identical with their antiparticles, is of fundamental importance for understanding the origin of ν-masses and mixing and the underlying symmetries of particle interactions (see *e.g.*, Ref. 51). The neutrinos with definite mass ν_j will be Dirac fermions if the particle interactions conserve some additive lepton number, *e.g.*, the total lepton charge $L = L_e + L_\mu + L_\tau$. If no lepton charge is conserved, ν_j will be Majorana fermions (see *e.g.*, Ref. 29). The massive neutrinos are predicted to be of Majorana nature by the see-saw mechanism of neutrino mass generation [3]. The observed patterns of neutrino mixing and of neutrino mass squared differences can be related to Majorana massive neutrinos and the existence of an approximate symmetry in the lepton sector corresponding, *e.g.*, to the conservation of the lepton charge $L' = L_e - L_\mu - L_\tau$ [123]. Determining the nature of massive neutrinos ν_j is one of the fundamental and most challenging problems in the future studies of neutrino mixing.

The Majorana nature of massive neutrinos ν_j manifests itself in the existence of processes in which the total lepton charge L changes by two units: $K^+ \to \pi^- + \mu^+ + \mu^+$, $\mu^- + (A, Z) \to \mu^+ + (A, Z-2)$, *etc.* Extensive studies have shown that the only feasible experiments having the potential of establishing that the massive neutrinos are Majorana particles are at present the experiments searching for $(\beta\beta)_{0\nu}$-decay: $(A, Z) \to (A, Z+2) + e^- + e^-$ (see *e.g.*, Ref. 124). The observation of $(\beta\beta)_{0\nu}$-decay and the measurement of the corresponding half-life with sufficient accuracy, would not only be a proof that the total lepton charge is not conserved, but might also provide unique information on the i) type of neutrino mass spectrum (see, *e.g.*, Ref. 125), ii) Majorana phases in U [114,126] and iii) the absolute scale of neutrino masses (for details see Ref. 124 to Ref. 127 and references quoted therein).

Under the assumptions of 3-ν mixing, of massive neutrinos ν_j being Majorana particles, and of $(\beta\beta)_{0\nu}$-decay generated only by the (V-A) charged current weak interaction via the exchange of the three Majorana neutrinos ν_j having masses $m_j \lesssim$ few MeV, the $(\beta\beta)_{0\nu}$-decay amplitude has the form (see, *e.g.*, Ref. 29 and Ref. 124): $A(\beta\beta)_{0\nu} \cong < m > M$, where M is the corresponding nuclear matrix element which does not depend on the neutrino mixing parameters, and

$$\begin{aligned} |< m >| &= \left| m_1 U_{\rm e1}^2 + m_2 U_{\rm e2}^2 + m_3 U_{\rm e3}^2 \right| \\ &= \left| \left(m_1 c_{12}^2 + m_2 s_{12}^2 e^{i\alpha_{21}} \right) c_{13}^2 + m_3 s_{13}^2 e^{i(\alpha_{31} - 2\delta)} \right|, \end{aligned} \tag{13.87}$$

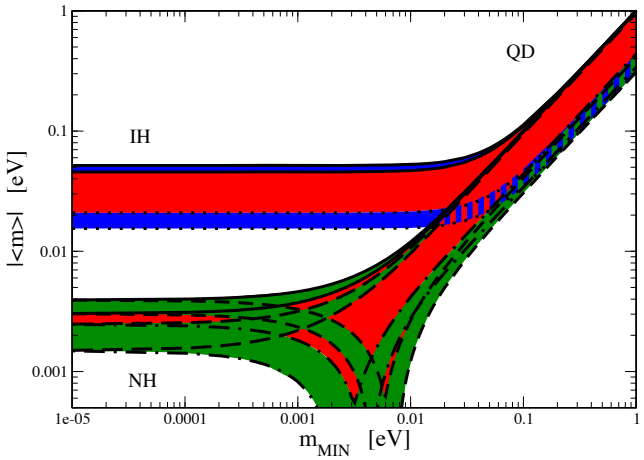

Figure 13.11: The effective Majorana mass $|<m>|$ (including a 2σ uncertainty) as a function of $\min(m_j)$. The figure is obtained using the best fit values and 1σ errors of Δm^2_{21}, $\sin^2\theta_{12}$, and $|\Delta m^2_{31}| \cong |\Delta m^2_{32}|$ from Ref. 112, fixed $\sin^2\theta_{13} = 0.01$ and $\delta = 0$. The phases $\alpha_{21,31}$ are varied in the interval $[0,\pi]$. The predictions for the NH, IH and QD spectra are indicated. The black lines determine the ranges of values of $|<m>|$ for the different pairs of CP conserving values of $\alpha_{21,31}$: $(\alpha_{21},\alpha_{31})=(0,0)$ solid, $(0,\pi)$ long dashed, $(\pi,0)$ dash-dotted, (π,π) short dashed, lines. The red regions correspond to at least one of the phases $\alpha_{21,31}$ and $(\alpha_{31}-\alpha_{21})$ having a CP violating value. (Update by S. Pascoli of a figure from the last article quoted in Ref. 127.)

is the effective Majorana mass in $(\beta\beta)_{0\nu}$-decay. In the case of CP-invariance one has [32], $\eta_{21} \equiv e^{i\alpha_{21}}=\pm 1$, $\eta_{31} \equiv e^{i\alpha_{31}}=\pm 1$, $e^{-i2\delta}=1$. The three neutrino masses $m_{1,2,3}$ can be expressed in terms of the two measured Δm^2_{jk} and, *e.g.*, $\min(m_j)$. Thus, given the neutrino oscillation parameters Δm^2_{21}, $\sin^2\theta_{12}$, Δm^2_{31} and $\sin^2\theta_{13}$, $|<m>|$ is a function of the lightest neutrino mass $\min(m_j)$, the Majorana (and Dirac) CP violation phases in U and of the type of neutrino mass spectrum. In the case of NH, IH and QD spectrum we have (see, *e.g.*, Ref. 114 and Ref. 127):

$$|<m>| \cong \left|\sqrt{\Delta m^2_{21}}s^2_{12}c^2_{13} + \sqrt{\Delta m^2_{31}}s^2_{13}e^{i(\alpha_{31}-\alpha_{21}-2\delta)}\right|, \quad \text{NH}, \tag{13.88}$$

$$|<m>| \cong \tilde{m}\left(1-\sin^2 2\theta_{12}\sin^2\frac{\alpha_{21}}{2}\right)^{\frac{1}{2}}, \quad \text{IH (IO) and QD}, \tag{13.89}$$

where $\tilde{m} \equiv \sqrt{\Delta m^2_{23}+m^2_3}$ and $\tilde{m} \equiv m_0$ for IH (IO) and QD spectrum, respectively. In Eq. (13.89) we have exploited the fact that $\sin^2\theta_{13} \ll \cos 2\theta_{12}$. The CP conserving values of the Majorana phases $(\alpha_{31}-\alpha_{21})$ and α_{21} determine the ranges of possible values of $|<m>|$, corresponding to the different types of neutrino mass spectrum. Using the best fit values of neutrino oscillation parameters, Eq. (13.78) to Eq. (13.80), and the upper limit on θ_{13}, Eq. (13.83), one finds that: i) $|<m>| \lesssim 0.005$ eV in the case of NH spectrum; ii) $\sqrt{\Delta m^2_{23}}\cos 2\theta_{12} \lesssim |<m>| \lesssim \sqrt{\Delta m^2_{23}}$, or 10^{-2} eV $\lesssim |<m>| \lesssim 0.05$ eV in the case of IH spectrum; iii) $m_0 \cos 2\theta_{12} \lesssim |<m>| \lesssim m_0$, or 0.03 eV $\lesssim |<m>| \lesssim m_0$ eV, $m_0 \gtrsim 0.10$ eV, in the case of QD spectrum. The difference in the ranges of $|<m>|$ in the cases of NH, IH and QD spectrum opens up the possibility to get information about the type of neutrino mass spectrum from a measurement of $|<m>|$ [125]. The predicted $(\beta\beta)_{0\nu}$-decay effective Majorana mass $|<m>|$ as a function of the lightest neutrino mass $\min(m_j)$ is shown in Fig. 13.11.

13.8. Outlook

After the spectacular experimental progress made in the studies of neutrino oscillations, further understanding of the pattern of neutrino masses and neutrino mixing, of their origins and of the status of CP symmetry in the lepton sector requires an extensive and challenging program of research. The main goals of such a research program include:

- Determining the nature - Dirac or Majorana, of massive neutrinos ν_j. This is of fundamental importance for making progress in our understanding of the origin of neutrino masses and mixing and of the symmetries governing the lepton sector of particle interactions.
- Determination of the sign of $\Delta m^2_{\rm A}$ (Δm^2_{31}) and of the type of neutrino mass spectrum.
- Determining or obtaining significant constraints on the absolute scale of neutrino masses.
- Measurement of, or improving by at least a factor of (5 - 10) the existing upper limit on, the small neutrino mixing angle θ_{13}. Together with the Dirac CP-violating phase, the angle θ_{13} determines the magnitude of CP-violation effects in neutrino oscillations.
- Determining the status of CP symmetry in the lepton sector.
- High precision measurement of Δm^2_{21}, θ_{12}, and $|\Delta m^2_{31}|$, θ_{23}.
- Understanding at a fundamental level the mechanism giving rise to neutrino masses and mixing and to L_l−non-conservation. This includes understanding the origin of the patterns of ν-mixing and ν-masses suggested by the data. Are the observed patterns of ν-mixing and of $\Delta m^2_{21,31}$ related to the existence of a new fundamental symmetry of particle interactions? Is there any relation between quark mixing and neutrino mixing, *e.g.*, does the relation $\theta_{12}+\theta_c=\pi/4$, where θ_c is the Cabibbo angle, hold? What is the physical origin of CP violation phases in the neutrino mixing matrix U? Is there any relation (correlation) between the (values of) CP violation phases and mixing angles in U? Progress in the theory of neutrino mixing might also lead to a better understanding of the mechanism of generation of baryon asymmetry of the Universe.

The successful realization of this research program would be a formidable task and would require many years. We are at the beginning of the "road" leading to a comprehensive understanding of the patterns of neutrino masses and mixing and of their origin.

References:

1. B. Pontecorvo, Zh. Eksp. Teor. Fiz. **53**, 1717 (1967) [Sov. Phys. JETP **26**, 984 (1968)].
2. M. Fukugita and T. Yanagida, Phys. Lett. **B174**, 45 (1986); V.A. Kuzmin, V.A. Rubakov, and M.E. Shaposhnikov, Phys. Lett. **B155**, 36 (1985).
3. P. Minkowski, Phys. Lett. **B67**, 421 (1977); see also: M. Gell-Mann, P. Ramond, and R. Slansky in *Supergravity*, p. 315, edited by F. Nieuwenhuizen and D. Friedman, North Holland, Amsterdam, 1979; T. Yanagida, *Proc. of the Workshop on Unified Theories and the Baryon Number of the Universe*, edited by O. Sawada and A. Sugamoto, KEK, Japan 1979; R.N. Mohapatra and G. Senjanović, Phys. Rev. Lett. **44**, 912 (1980).
4. B.T. Cleveland *et al.*, Astrophys. J. **496**, 505 (1988).
5. Y. Fukuda *et al.*, [Kamiokande Collab.], Phys. Rev. Lett. **77**, 1683 (1996).
6. J.N. Abdurashitov *et al.*, Phys. Rev. **C80**, 015807 (2009).
7. P. Anselmann *et al.*, Phys. Lett. **B285**, 376 (1992).
8. W. Hampel *et al.*, Phys. Lett. **B447**, 127 (1999).
9. M. Altmann *et al.*, Phys. Lett. **B616**, 174 (2005).
10. S. Fukuda *et al.*, [Super-Kamiokande Collab.], Phys. Lett. **B539**, 179 (2002).
11. Q.R. Ahmad *et al.*, [SNO Collab.], Phys. Rev. Lett. **87**, 071301 (2001).
12. Q.R. Ahmad *et al.*, [SNO Collab.], Phys. Rev. Lett. **89**, 011301 (2002).

13. Y. Fukuda *et al.*, [Super-Kamiokande Collab.], Phys. Rev. Lett. **81**, 1562 (1998).
14. Y. Ashie *et al.*, [Super-Kamiokande Collab.], Phys. Rev. Lett. **93**, 101801 (2004).
15. K. Eguchi *et al.*, [KamLAND Collab.], Phys. Rev. Lett. **90**, 021802 (2003).
16. T. Araki *et al.*, [KamLAND Collab.], Phys. Rev. Lett. **94**, 081801 (2005).
17. B. Pontecorvo, Zh. Eksp. Teor. Fiz. **33**, 549 (1957) and **34**, 247 (1958).
18. Z. Maki, M. Nakagawa, and S. Sakata, Prog. Theor. Phys. **28**, 870 (1962).
19. D. Karlen in RPP2010.
20. M.H. Ahn *et al.*, [K2K Collab.], Phys. Rev. **D74**, 072003 (2006).
21. D.G. Michael *et al.*, [MINOS Collab.], Phys. Rev. Lett. **97**, 191801 (2006).
22. P. Adamson *et al.*, [MINOS Collab.], Phys. Rev. Lett. **101**, 131802 (2008).
23. A. Aguilar *et al.*, Phys. Rev. **D64**, 112007 (2001).
24. A.A. Aguilar-Arevalo *et al.*, Phys. Rev. Lett. **98**, 231801 (2007).
25. L. Wolfenstein, Phys. Rev. **D17**, 2369 (1978).
26. S.P. Mikheev and A.Y. Smirnov, Sov. J. Nucl. Phys. **42**, 913 (1985); Nuovo Cimento **9C**, 17 (1986).
27. E. Majorana, Nuovo Cimento **5**, 171 (1937).
28. Majorana particles, in contrast to Dirac fermions, are their own antiparticles. An electrically charged particle (like the electron) cannot coincide with its antiparticle (the positron) which carries the opposite non-zero electric charge.
29. S.M. Bilenky and S.T. Petcov, Rev. Mod. Phys. **59**, 671 (1987).
30. S.M. Bilenky, J. Hosek, and S.T. Petcov, Phys. Lett. **B94**, 495 (1980).
31. J. Schechter and J.W.F. Valle, Phys. Rev. **D23**, 2227 (1980); M. Doi *et al.*, Phys. Lett. **B102**, 323 (1981).
32. L. Wolfenstein, Phys. Lett. **B107**, 77 (1981); S.M. Bilenky, N.P. Nedelcheva, and S.T. Petcov, Nucl. Phys. **B247**, 61 (1984); B. Kayser, Phys. Rev. **D30**, 1023 (1984).
33. S. Nussinov, Phys. Lett. **B63**, 201 (1976); B. Kayser, Phys. Rev. **D24**, 110 (1981); J. Rich, Phys. Rev. **D48**, 4318 (1993); H. Lipkin, Phys. Lett. **B348**, 604 (1995); W. Grimus and P. Stockinger, Phys. Rev. **D54**, 3414 (1996); L. Stodolski, Phys. Rev. **D58**, 036006 (1998); W. Grimus, P. Stockinger, and S. Mohanty, Phys. Rev. **D59**, 013011 (1999); L.B. Okun, Surv. High Energy Physics **15**, 75 (2000); J.-M. Levy, `hep-ph/0004221` and `arXiv:0901.0408`; A.D. Dolgov, Phys. Reports **370**, 333 (2002); C. Giunti, Phys. Scripta **67**, 29 (2003) and Phys. Lett. **B17**, 103 (2004); M. Beuthe, Phys. Reports **375**, 105 (2003); H. Lipkin, Phys. Lett. **B642**, 366 (2006); S.M. Bilenky, F. von Feilitzsch, and W. Potzel, J. Phys. **G34**, 987 (2007); C. Giunti and C.W. Kim, *Fundamentals of Neutrino Physics and Astrophysics* (Oxford University Press, Oxford, 2007); E.Kh. Akhmedov, J. Kopp, and M. Lindner, JHEP **0805**, 005 (2008); E.Kh. Akhmedov and A.Yu. Smirnov, Phys. Atom. Nucl. **72**, 1363 (2009).
34. For the subtleties involved in the step leading from Eq. (13.1) to Eq. (13.5) see, *e.g.*, Ref. 35.
35. A.G. Cohen, S.L. Glashow, and Z. Ligeti, `arXiv:0810.4602`.
36. The neutrino masses do not exceed approximately 1 eV, $m_j \lesssim 1$, while in neutrino oscillation experiments neutrinos with energy $E \gtrsim 100$ keV are detected.
37. S.M. Bilenky and B. Pontecorvo, Phys. Reports **41**, 225 (1978).
38. In Eq. (13.9) we have neglected the possible instability of neutrinos ν_j. In most theoretical models with nonzero neutrino masses and neutrino mixing, the predicted half life-time of neutrinos with mass of 1 eV exceeds the age of the Universe, see, *e.g.*, S.T. Petcov, Yad. Fiz. **25**, 641 (1977), (E) *ibid.*, **25** (1977) 1336 [Sov. J. Nucl. Phys. **25**, 340 (1977), (E) *ibid.*, **25**, (1977), 698], and Phys. Lett. **B115**, 401 (1982); W. Marciano and A.I. Sanda, Phys. Lett. **B67**, 303 (1977); P. Pal and L. Wolfenstein, Phys. Rev. **D25**, 766 (1982).
39. L.B. Okun (2000), J.-M. Levy (2000) and H. Lipkin (2006) quoted in Ref. 33 and Ref. 35.
40. The articles by L. Stodolsky (1998) and H. Lipkin (1995) quoted in Ref. 33.
41. V. Gribov and B. Pontecorvo, Phys. Lett. **B28**, 493 (1969).
42. N. Cabibbo, Phys. Lett. **B72**, 333 (1978).
43. V. Barger *et al.*, Phys. Rev. Lett. **45**, 2084 (1980).
44. P. Langacker *et al.*, Nucl. Phys. **B282**, 589 (1987).
45. P.I. Krastev and S.T. Petcov, Phys. Lett. **B205**, 84 (1988).
46. C. Jarlskog, Z. Phys. **C29**, 491 (1985).
47. A. De Rujula *et al.*, Nucl. Phys. **B168**, 54 (1980).
48. S. Goswami *et al.*, Nucl. Phys. (Proc. Supp.) **B143**, 121 (2005).
49. These processes are important, however, for the supernova neutrinos see, *e.g.*, G. Raffelt, *Proc. International School of Physics "Enrico Fermi", CLII Course "Neutrino Physics"*, 23 July-2 August 2002, Varenna, Italy [`hep-ph/0208024`]), and articles quoted therein.
50. We standardly assume that the weak interaction of the flavour neutrinos ν_l and antineutrinos $\bar{\nu}_l$ is described by the Standard Model (for alternatives see, *e.g.*, [25]; M.M. Guzzo *et al.*, Phys. Lett. **B260**, 154 (1991); E. Roulet, Phys. Rev. **D44**, R935 (1991) and Ref. 51).
51. R. Mohapatra *et al.*, Rept. on Prog. in Phys. **70**, 1757 (2007); A. Bandyopadhyay *et al.*, Rept. on Prog. in Phys. **72**, 106201 (2009).
52. V. Barger *et al.*, Phys. Rev. **D22**, 2718 (1980).
53. P. Langacker, J.P. Leveille, and J. Sheiman, Phys. Rev. **D27**, 1228 (1983).
54. The difference between the ν_μ and ν_τ indices of refraction arises at one-loop level and can be relevant for the $\nu_\mu - \nu_\tau$ oscillations in very dense media, like the core of supernovae, *etc.*; see F.J. Botella, C.S. Lim, and W.J. Marciano, Phys. Rev. **D35**, 896 (1987).
55. The relevant formulae for the oscillations between the ν_e and a sterile neutrino ν_s, $\nu_e \leftrightarrow \nu_s$, can be obtained from those derived for the case of $\nu_e \leftrightarrow \nu_{\mu(\tau)}$ oscillations by [44,53] replacing N_e with $(N_e - 1/2N_n)$, N_n being the neutron number density in matter.
56. T.K. Kuo and J. Pantaleone, Phys. Lett. **B198**, 406 (1987).
57. A.D. Dziewonski and D.L. Anderson, Physics of the Earth and Planetary Interiors **25**, 297 (1981).
58. The first studies of the effects of Earth matter on the oscillations of neutrinos were performed numerically in [52,59] and in E.D. Carlson, Phys. Rev. **D34**, 1454 (1986); A. Dar *et al.*, *ibid.*, **D35**, 3607 (1988); in [45] and in G. Auriemma *et al.*, *ibid.*, **D37**, 665 (1988).
59. A.Yu. Smirnov and S.P. Mikheev, *Proc. of the VIth Moriond Workshop* (eds. O. Fackler, J. Tran Thanh Van, Frontières, Gif-sur-Yvette, 1986), p. 355.
60. S.T. Petcov, Phys. Lett. **B434**, 321 (1998), (E) *ibid.* **B444**, 584 (1998).
61. S.T. Petcov, Phys. Lett. **B214**, 259 (1988); "Earth Matter Effects in the Atmospheric and Solar Neutrino Transitions," Talk given at the Workshop "Neutrino Physics and Astrophysics," Aspen Center for Physics, June 29 - July 12, 1998, Aspen, U.S.A.
62. E.Kh. Akhmedov *et al.*, Nucl. Phys. **B542**, 3 (1999).
63. M.V. Chizhov, M. Maris, and S.T. Petcov, `hep-ph/9810501`; see also: S.T. Petcov, Nucl. Phys. (Proc. Supp.) **B77**, 93 (1999) (`hep-ph/9809587`).
64. J. Hosaka *et al.*, [Super-Kamiokande collab.], Phys. Rev. **D74**, 032002 (2006).
65. E.Kh. Akhmedov, Nucl. Phys. **B538**, 25 (1999).
66. M.V. Chizhov and S.T. Petcov, Phys. Rev. Lett. **83**, 1096 (1999) and Phys. Rev. Lett. **85**, 3979 (2000); Phys. Rev. **D63**, 073003 (2001).
67. J. Bernabéu, S. Palomares-Ruiz, and S.T. Petcov, Nucl. Phys. **B669**, 255 (2003); S.T. Petcov and T. Schwetz, Nucl. Phys. **B740**, 1 (2006); R. Gandhi *et al.*, Phys. Rev. **D76**, 073012 (2007); E.Kh. Akhmedov, M. Maltoni, and A.Yu. Smirnov, JHEP **0705**, 077 (2007).

68. The mantle-core enhancement maxima, *e.g.*, in $P_m^{2\nu}(\nu_\mu \to \nu_\mu)$, appeared in some of the early numerical calculations, but with incorrect interpretation (see, *e.g.*, the articles quoted in Ref. 58).
69. M. Freund, Phys. Rev. **D64**, 053003 (2001).
70. M.C. Gonzalez-Garcia and Y. Nir, Rev. Mod. Phys. **75**, 345 (2003); S.M. Bilenky, W. Grimus, and C. Giunti, Prog. in Part. Nucl. Phys. **43**, 1 (1999); S.T. Petcov, Lecture Notes in Physics **512**, (eds. H. Gausterer, C.B. Lang, Springer, 1998), p. 281.
71. J.N. Bahcall, *Neutrino Astrophysics*, Cambridge University Press, Cambridge, 1989; J.N. Bahcall and M. Pinsonneault, Phys. Rev. Lett. **92**, 121301 (2004).
72. J.N. Bahcall, A.M. Serenelli, and S. Basu, Astrophys. J. Supp. **165**, 400 (2006).
73. A. Messiah, *Proc. of the VIth Moriond Workshop* (eds. O. Fackler, J. Tran Thanh Van, Frontières, Gif-sur-Yvette, 1986), p. 373.
74. S.J. Parke, Phys. Rev. Lett. **57**, 1275 (1986).
75. S.T. Petcov, Phys. Lett. **B200**, 373 (1988).
76. P.I. Krastev and S.T. Petcov, Phys. Lett. **B207**, 64 (1988); M. Bruggen, W.C. Haxton, and Y.-Z. Quian, Phys. Rev. **D51**, 4028 (1995).
77. T. Kaneko, Prog. Theor. Phys. **78**, 532 (1987); S. Toshev, Phys. Lett. **B196**, 170 (1987); M. Ito, T. Kaneko, and M. Nakagawa, Prog. Theor. Phys. **79**, 13 (1988), (E) *ibid.*, **79**, 555 (1988).
78. S.T. Petcov, Phys. Lett. **B406**, 355 (1997).
79. C. Cohen-Tannoudji, B. Diu, and F. Laloe, *Quantum Mechanics*, vol. 1 (Hermann, Paris, and John Wiley & Sons, New York, 1977).
80. S.T. Petcov, Phys. Lett. **B214**, 139 (1988); E. Lisi *et al.*, Phys. Rev. **D63**, 093002 (2000); A. Friedland, Phys. Rev. **D64**, 013008 (2001).
81. S.T. Petcov and J. Rich, Phys. Lett. **B224**, 401 (1989).
82. An expression for the "jump" probability P' for N_e varying linearly along the neutrino path was derived in W.C. Haxton, Phys. Rev. Lett. **57**, 1271 (1986) and in Ref. 74 on the basis of the old Landau-Zener result: L.D. Landau, Phys. Z. USSR **1**, 426 (1932), C. Zener, Proc. R. Soc. A **137**, 696 (1932). An analytic description of the solar ν_e transitions based on the Landau-Zener jump probability was proposed in Ref. 74 and in W.C. Haxton, Phys. Rev. **D35**, 2352 (1987). The precision limitations of this description, which is less accurate than that based on the exponential density approximation, were discussed in S.T. Petcov, Phys. Lett. **B191**, 299 (1987) and in Ref. 76.
83. A. de Gouvea, A. Friedland, and H. Murayama, JHEP **0103**, 009 (2001).
84. C.-S. Lim, Report BNL 52079, 1987; S.P. Mikheev and A.Y. Smirnov, Phys. Lett. **B200**, 560 (1988).
85. G.L. Fogli *et al.*, Phys. Lett. **B583**, 149 (2004).
86. J.N. Bahcall, A.M. Serenelli, and S. Basu, Astrophys. J. **621**, L85 (2005).
87. C. Peña-Garay and A.M. Serenelli, `arXiv:0811.2424`.
88. B. Pontecorvo, Chalk River Lab. report PD-205, 1946.
89. D. Davis, Jr., D.S. Harmer, and K.C. Hoffman, Phys. Rev. Lett. **20**, 1205 (1968).
90. A.I. Abazov *et al.*, Phys. Rev. Lett. **67**, 3332 (1991).
91. K.S. Hirata *et al.*, Phys. Rev. Lett. **63**, 16 (1989).
92. Y. Fukuda *et al.*, Phys. Rev. Lett. **81**, 1158 (1998).
93. J. Hosaka *et al.*, Phys. Rev. **D73**, 112001 (2006).
94. B. Aharmim *et al.*, Phys. Rev. **C72**, 055502 (2005).
95. B. Aharmim *et al.*, Phys. Rev. Lett. **101**, 111301 (2008).
96. C. Arpesella *et al.*, Phys. Lett. **B658**, 101 (2008); Phys. Rev. Lett. **101**, 091302 (2008).
97. B. Aharmim *et al.*, `arXiv:0910.2984`.
98. Y. Fukuda *et al.*, Phys. Rev. Lett. **86**, 5651 (2001).
99. Y. Fukuda *et al.*, Phys. Lett. **B539**, 179 (2002).
100. G. L. Fogli *et al.*, Phys. Rev. **D67**, 073002 (2003); M. Maltoni, T. Schwetz, and J.W. Valle, Phys. Rev. **D67**, 093003 (2003); A. Bandyopadhyay *et al.*, Phys. Lett. **B559**, 121 (2003); J.N. Bahcall, M.C. Gonzalez-Garcia, and C. Peña-Garay, JHEP **0302**, 009 (2003); P.C. de Holanda and A.Y. Smirnov, JCAP **0302**, 001 (2003).
101. S. Abe *et al.*, Phys. Rev. Lett. **100**, 221803 (2008).
102. Y. Ashie *et al.*, Phys. Rev. **D71**, 112005 (2005).
103. K. Abe *et al.*, Phys. Rev. Lett. **97**, 171801 (2006).
104. V. Barger *et al.*, Phys. Rev. Lett. **82**, 2640 (1999).
105. E. Lisi *et al.*, Phys. Rev. Lett. **85**, 1166 (2000).
106. M. Guler *et al.*, [OPERA Collab.], CERN/SPSC 2000-028 (2000).
107. M. Apollonio *et al.*, Phys. Lett. **B466**, 415 (1999); Eur. Phys. J. **C27**, 331 (2003).
108. F. Boehm *et al.*, Phys. Rev. Lett. **84**, 3764 (2000); Phys. Rev. **D64**, 112001 (2001).
109. S. Yamamoto *et al.*, Phys. Rev. Lett. **96**, 181801 (2006).
110. G.L. Fogli *et al.*, Phys. Rev. Lett. **101**, 141801 (2008).
111. G.L. Fogli *et al.*, Phys. Rev. **D78**, 033010 (2008).
112. T. Schwetz, M. Tórtola, and J.W. F. Valle, `arXiv:0808.2016`.
113. In the convention we use, the neutrino masses are not ordered in magnitude according to their index number: $\Delta m^2_{31} < 0$ corresponds to $m_3 < m_1 < m_2$. We can also number the massive neutrinos in such a way that one always has $m_1 < m_2 < m_3$, see, *e.g.*, Ref. 114.
114. S.M. Bilenky, S. Pascoli, and S.T. Petcov, Phys. Rev. **D64**, 053010 (2001) and *ibid.*, 113003; S.T. Petcov, Physica Scripta **T121**, 94 (2005).
115. F. Perrin, Comptes Rendus **197**, 868 (1933); E. Fermi, Nuovo Cim. **11**, 1 (1934).
116. V. Lobashev *et al.*, Nucl. Phys. **A719**, 153c, (2003).
117. K. Eitel *et al.*, Nucl. Phys. (Proc. Supp.) **B143**, 197 (2005).
118. D.N. Spergel *et al.*, Astrophys. J. Supp. **170**, 377 (2007).
119. M. Fukugita *et al.*, Phys. Rev. **D74**, 027302 (2006).
120. S. Davidson and A. Ibarra, Phys. Lett. **B535**, 25 (2002).
121. A. Abada *et al.*, JCAP **0604**, 004 (2006); E. Nardi *et al.*, JHEP **0601**, 164 (2006).
122. S. Pascoli, S.T. Petcov, and A. Riotto, Phys. Rev. **D75**, 083511 (2007) and Nucl. Phys. **B774**, 1 (2007); E. Molinaro and S.T. Petcov, Phys. Lett. **B671**, 60 (2009).
123. S.T. Petcov, Phys. Lett. **B110**, 245 (1982); R. Barbieri *et al.*, JHEP **9812**, 017 (1998); P.H. Frampton, S.T. Petcov, and W. Rodejohann, Nucl. Phys. **B687**, 31 (2004).
124. A. Morales and J. Morales, Nucl. Phys. (Proc. Supp.) **B114**, 141 (2003); C. Aalseth *et al.*, `hep-ph/0412300`; S.R. Elliott and P. Vogel, Ann. Rev. Nucl. Part. Sci. **52**, 115 (2002).
125. S. Pascoli and S.T. Petcov, Phys. Lett. **B544**, 239 (2002); *ibid.*, **B580**, 280 (2004); see also: S. Pascoli, S.T. Petcov, and L. Wolfenstein, Phys. Lett. **B524**, 319 (2002).
126. S.M. Bilenky *et al.*, Phys. Rev. **D54**, 4432 (1996).
127. S.M. Bilenky *et al.*, Phys. Lett. **B465**, 193 (1999); F. Vissani, JHEP **06**, 022 (1999); K. Matsuda *et al.*, Phys. Rev. **D62**, 093001 (2000); K. Czakon *et al.*, `hep-ph/0003161`; H.V. Klapdor-Kleingrothaus, H. Päs and A.Yu. Smirnov, Phys. Rev. **D63**, 073005 (2001) S. Pascoli, S.T. Petcov and W. Rodejohann, Phys. Lett. **B549**, 177 (2002), and *ibid.* **B558**, 141 (2003); H. Murayama and Peña-Garay, Phys. Rev. **D69**, 031301 (2004); S. Pascoli, S.T. Petcov, and T. Schwetz, Nucl. Phys. **B734**, 24 (2006); M. Lindner, A. Merle, and W. Rodejohann, Phys. Rev. **D73**, 053005 (2006); A. Faessler *et al.*, Phys. Rev. **D79**, 053001 (2009); S. Pascoli and S.T. Petcov, Phys. Rev. **D77**, 113003 (2008).